Full title: **Characterizing the secret diets of siphonophores (Cnidaria: Hydrozoa) using DNA metabarcoding**

Short title: **Siphonophore diets using DNA metabarcoding**

Alejandro Damian-Serrano[1,2], Elizabeth D. Hetherington[3], C. Anela Choy[3], Steven H.D. Haddock[4], Alexandra Lapides[4], Casey W. Dunn[1]

[1] Yale University, Department of Ecology and Evolutionary Biology, 165 Prospect St., New Haven, CT 06520, USA

[2] Institute of Ecology and Evolution, University of Oregon, 1318 Franklin Blvd., Eugene, OR, 97401, USA

[3] Scripps Institution of Oceanography, University of California San Diego, Integrative Oceanography Division, 9500 Gilman Drive, La Jolla, CA 92037, USA

[4] Monterey Bay Aquarium Research Institute, Midwater Research, 7700 Sandholdt Rd., Moss Landing, CA 95039, USA

Corresponding author: Alejandro Damian-Serrano (email: adamians@uoregon.edu)

Abstract

Siphonophores (Cnidaria: Hydrozoa) are abundant and diverse gelatinous predators in open-ocean ecosystems. Due to limited access to the midwater, little is known about the diets of most deep-dwelling gelatinous species, which constrains our understanding of food-web structure and nutrient flow in these vast ecosystems. Visual gut-content methods can rarely identify soft-bodied rapidly-digested prey, while observations from submersibles often overlook small prey items. These methods have been differentially applied to shallow and deep siphonophore taxa, confounding habitat and methodological biases. DNA metabarcoding can be used to assess both shallow and deep species' diets under a common methodological framework, since it can detect both small and gelatinous prey. We (1) further characterized the diets of open-ocean siphonophores using DNA metabarcoding, (2) compared the prey detected by visual and molecular methods to evaluate their technical biases, and (3) evaluated tentacle-based predictions of diet. To do this, we performed DNA metabarcoding analyses on the gut contents of 39 siphonophore species across depths to describe their diets, using six barcode regions along the 18S gene. Taxonomic identifications were assigned using public databases combined with local zooplankton sequences. We identified 55 unique prey items, including crustaceans, gelatinous animals, and fish across 47 siphonophore specimens in 24 species. We reported 29 novel predator-prey interactions, among them the first insights into the diets of nine siphonophore species, many of which were congruent with the dietary predictions based on tentilla morphology. Our analyses detected small prey and gelatinous prey taxa underrepresented by visual methods in species from both shallow and deep habitats, revealing hidden links between siphonophores and filter-feeders near the base of the food web. This study expands our understanding of the ecological roles of siphonophores in the open ocean, their trophic roles within the 'jelly-web', and the importance of their diversity for nutrient flow and ecosystem functioning. Understanding these

inconspicuous yet ubiquitous predator-prey interactions is critical to predict the impacts of climate change, overfishing, and conservation policies on oceanic ecosystems.

Keywords

Gelatinous zooplankton, trophic ecology, predator-prey interactions, pelagic food webs, siphonophores

Introduction

The open-ocean midwater is the largest volume of the biosphere habitable by animals (Harbison 1992). This environment hosts diverse communities and complex food webs (Robison 2004). Midwater food webs sustain manifold fisheries, top predators, and sustain the biological carbon pump (Falkowski et al. 1998). Gelatinous animals play fundamental roles in these food webs (Choy et al. 2017), acting as herbivores, predators, and prey. The subset of the midwater food web involving gelatinous fauna has been referred to as the “jelly web” (Robison 2004). Among the most abundant (O’Brien 2007, Grossman et al. 2015) and trophically-connected (Choy et al. 2017) gelatinous predators are siphonophores — mid-trophic organisms that feed on a broad variety of prey such as medusae, salps, crustaceans, molluscs, and fishes (Purcell 1981a, Choy et al. 2017, Hetherington et al. in review). Siphonophores are sit-and-wait, non-visual, ambush predators that rely on prey encountering their tentacles and tentilla (Mackie et al. 1988). They are abundant and locally diverse colonial cnidarians in open-ocean communities, present in every region of the ocean, with species ranging from above the surface (like the Portuguese man-o-war) to the hadal region (>7000m deep) (Jamieson and Linley 2021). In addition, siphonophore aggregations can have significant predatory impacts on larval fish stocks (Purcell 1981b).

Progress in elucidating siphonophore diets has been slow due to the intrinsic challenges of working with these animals. Observation and collection of open-ocean taxa requires expensive research vessels and instrumentation to reach their habitat. In addition, siphonophores are

extremely fragile, requiring the use of blue water SCUBA divers and Remotely Operated Vehicles (ROVs) to collect them alive and intact (Haddock 2004). These techniques can be used to collect live specimens for gut content inspection, and video recordings from ROVs allow scientists to observe feeding events. Traditional collection methods such as plankton nets not only break up siphonophore colonies, but can also lead to artifactual ingestions in the cod-end that confound their natural diets.

The diets of some epipelagic siphonophores have been examined through gut content analyses of SCUBA-collected colonies (Biggs 1977, Purcell 1981a, reviewed in Hetherington et al. in review). Recent studies based on ROV observations have shed some light on the diets of deep midwater siphonophores (Choy et al. 2017, Hetherington et al. in review). However, these approaches are limited by their biases. Visual gut content inspection favors hard-bodied prey that digest slowly, leaving behind diagnostic body parts (i.e. exoskeleton, shell, eyes, etc.). Therefore, soft-bodied, rapidly-digested taxa, such as gelatinous zooplankton, are often underrepresented in dietary assessments. ROVs can observe feeding on gelatinous prey before they become digested. However, ROV observations are skewed towards large prey items that can be easily identified from the camera screen (such as large medusae, ctenophores, crustaceans, or fishes), and can overlook important prey items such as copepods and larvae (Hetherington et al. in review). In addition, prey are relatively scarce in the open ocean, especially in the deeper regions (Robison 2004), thus it is infrequent to find specimens capturing prey or carrying visually-identifiable prey in their guts (Purcell, 1981a).

With the advent of DNA metabarcoding, the diets of many marine predators have been established from gut content DNA (Leray et al. 2013, Harms-Tuohy et al. 2016, Fernández-Álvarez et al. 2018, Reis et al. 2018). These high-throughput amplicon sequencing technologies have extremely high detection sensitivity and bypass the biases posed by visual methods. Recently, the application of DNA metabarcoding to marine predator gut contents has

demonstrated the capacity of these methods to detect gelatinous prey (Connell et al. 2014, McInnes et al. 2017, Clarke et al. 2018, Jensen et al. 2018, Marques et al. 2019). However, this technology has not yet been applied to study the diets of gelatinous animals.

In Hetherington et al. (in review), we reviewed and summarized the literature on siphonophore diets, and observed significant differences between the diets of epipelagic and deep-dwelling siphonophore species. Gelatinous prey appeared to be more prevalent in deep-sea observations while small crustaceans appeared to be the predominant prey in shallow gut content samples. Since epipelagic species' diets were exclusively assessed through microscopic gut content inspection and deep-sea species' diets through ROV observations, it is not possible to determine whether these differences are due to ecological or methodological reasons. To disentangle these confounding factors, it is critical to assess both shallow and deep species' diets under the same methodological framework. In this case, DNA metabarcoding is an ideal choice, since it can detect both small and gelatinous prey, thus being able to bridge across the methodological shortcomings of visual methods. Here we aim to apply a uniform method to describe diets across the water column as a single, interconnected, deep-pelagic ecosystem.

Siphonophore tentillum and nematocyst morphology are directly linked to feeding guild (Damian Serrano et al. 2021a). Damian-Serrano et al. (2021b) used these relationships to generate feeding guild predictions for 45 siphonophore species using their tentillum and nematocyst morphology as predictors. The feeding guild categories comprise fish specialists (which feed primarily on teleost fish prey), large crustacean specialists (which feed primarily on krill, decapod shrimps, mysids, lophogastrids, amphipods, and other macro-planktonic crustaceans larger than 1cm), small crustacean specialists (which feed primarily on copepods, ostracods, cladocerans, larvae, and other meso-planktonic crustaceans smaller than 1cm), gelatinous specialists (which are able to feed on large gelatinous animals such as salps, ctenophores, or medusae in addition to other zooplankton), and generalists (which feed on a

variety of small and large, soft- and hard-bodied prey not including gelatinous animals). These predictions were cast on siphonophore species for which no dietary information was available, and thus remained to be tested with new data on siphonophore diets.

Here we use DNA metabarcoding to identify the gut contents of several siphonophore species to obtain more comprehensive insights into their diets. Our primary aims are: (1) Expand the existing knowledge on the diets of open-ocean siphonophores using DNA metabarcoding, (2) qualitatively compare the prey detected by visual and molecular methods to evaluate their technical biases, (3) apply a uniform method to describe siphonophore diets across depth habitats, and (4) evaluate the morphology-based predictions of feeding guilds.

Results and Discussion

We extracted, amplified, and sequenced the gut contents of 159 specimens from 41 siphonophore species. We obtained a total of 4148 unique sequences, including 1502 sequences from region “134”, 614 from region “152”, 758 from region “166”, 497 from region “179”, and 341 from region “261”, and 442 from region “272” (Fig. 3, SM-Figures 5 and 9). A total of 337 unique sequences were interpreted as prey items, 36 as secondary predation, 292 as contamination from extrinsic sources, 2857 as natural environmental DNA sources, 791 as siphonophore sequences, 85 as parasites (myxozoans, trematodes, and other helminths), and 14 unrecognizable sequences. We identified prey items in 47 specimens (~30%) from 24 siphonophore species (Fig. 3, SM-Figures 10-12). This prevalence of empty guts is consistent with the feeding habits of macrophagous sit-and-wait ambush predators in oligotrophic environments, with scarce feeding events separated by periods of starvation (Griffiths 1975). We identified 55 unique prey items, 42 of which were crustaceans (25 of which were copepods), three of them were fishes, four of them were thaliaceans, five corresponded to other gelatinous predators (ctenophores and a medusa), and one matching to a bivalve mollusc (SM-Figure 1). Most (112 out of 159) siphonophore specimens collected did not yield any putative prey taxaconcepts (Fig. 2). Among the 47

specimens with prey, 40 of them had DNA from a single prey item, while only six had two prey items, and one *Apolemia* sp. specimen had three prey items (SM-Figure 1). The use of six different barcode regions (within the 18S gene) allowed us to detect a broader taxonomic range of prey and to validate dubious annotations (Fig. 3).

Dietary findings by taxon

Physalia physalis — The Portuguese man-o-war is the only pleustonic (surface floating) member of the siphonophores, and the most encountered by beachgoers. Man-o-wars are well-known to feed exclusively on relatively large and motile soft-bodied prey such as fish, chaetognaths, or pelagic gastropods (Purcell 1984a). In our gut content samples of the Portuguese man-o-war from Bermuda, we found three specimens with ray-finned fish sequences, some of which had visually recognizable fish in the gastrozooids when collected. Fish prey is congruent with published visual inspections of their gut contents (Purcell 1984a, Bardi & Marques 2007). In all three specimens with fish prey we also found benthic and hard-bodied taxa (mysid, alpheid shrimp, spider crab, copepod, benthic gastropod, and a sipunculid worm), as well as larvacean prey sequences. Their nematocysts are not able to subdue crustacean prey, and their feeding reflex would not be triggered by a prey as small as a larvacean (Purcell 1984b). Therefore, we interpreted the presence of these taxa in the gut contents as secondary predation in the gut contents of the fish prey (SM-Figures 3 and 7). In addition, we also detected ctenophore prey in one specimen. This could be also a case of secondary predation, but we suspect a ctenophore could be large enough to be prey of the man-o-war. If that is the case, this would be the first record of *P. physalis* consuming gelatinous zooplankton, which would place the man-o-war as a central species in the epipelagic 'jelly-web' (Chi et al. 2020). Comparisons with their surrounding prey field show these specimens were strongly selective for fish and strongly exclusive of copepods (Fig. 4).

Apolemia spp. — These are among the longest siphonophores, with colonies attaining lengths as long as 30m (Mackie et al. 1988). Their tentacles are different from other siphonophores since they have no tentilla and carry birhopaloid nematocysts directly on the tentacles (Damian-Serrano et al. 2021b). *Apolemia* species are known to consume diverse prey including crustaceans, molluscs, polychaetes, chaetognaths, fish, and gelatinous zooplankton (Purcell 1981a, Choy et al. 2017). While this may suggest these species are generalists, Damian-Serrano et al. (2021a) hypothesized that they may be gelatinous zooplankton specialists, since they consume a larger proportion of this prey type than other siphonophores. In addition, the nematocysts of *Apolemia* have similar traits to those in other gelativorous cnidarians (Purcell & Mills 1988), and their apparent generality could be explained by the sheer number of fine tentacles deployed for prey capture per colony, which would inevitably entangle almost anything that swims by. All species of *Apolemia* analyzed here had consumed copepods, the *A. rubriversa* specimen had also consumed a salp, and the undescribed *Apolemia* species also had ctenophore, larvacean, mysid, and euphausiid prey sequences (Figs. 2-4). The salp prey found in *A. rubriversa* is congruent with its characterization as a gelatinous specialist in Damian-Serrano et al. (2021a). While the morphology-based predictions derived from Damian-Serrano et al. (2021b) indicate that *A. lanosa* is a gelatinous prey specialist, we only found copepod prey in our sample. However, it is possible that the doliolid and hydromedusa reads we conservatively labelled as potential cross-contamination could correspond to real prey. Considering the differences we found between species, it seems possible that these coexisting species of midwater *Apolemia* are partitioning their trophic niche by varying the proportion of crustacean versus gelatinous prey they consume. Moreover, the salp prey found in *A. rubriversa* indicates a direct connection between phytoplankton consumers and siphonophores.

Bargmannia spp. — The three *Bargmannia* species considered here are frequently-observed in the midwaters off Monterey Bay, and have relatively simple tentilla with large

stenotele nematocysts and an undifferentiated terminal filament (Damian-Serrano et al. 2021b). ROVs have recorded *Bargmannia elongata* consuming crustaceans and cephalopods, and during specimen collection we observed a mysid prey in a specimen *Bargmannia amoena*. Nothing was previously known, however, about the diet of *Bargmannnia lata*. DNA metabarcoding confirmed the identity of the mysid in *B. amoena* as *Boreomysis californica*, and found a copepod in another specimen. One *B. elongata* specimen had euphausiid and ostracod prey, in agreement with the DAPC prediction for *B. elongata* to feed mainly on large crustaceans, but also marginally on small crustaceans. The two *B. lata* specimens consumed a ctenophore and a copepod, respectively. The diets of these three closely-related, coexisting species appear to be non-overlapping, which could be a consequence of competitive trophic niche partitioning. The findings for *B. lata* are not congruent with the morphology-based prediction to be a large-crustacean specialist (Fig. 5). We suspect that the lack of taxon sampling among the pyrostephids in Damian-Serrano et al. (2021a) could have led to overfitting in the DAPC. Finding ctenophore prey also supports the involvement of deep-sea siphonophores in the midwater 'jelly web'.

Other deep-sea physonects — Undescribed physonect sp. L was predicted to be a fish specialist with a secondary affinity for large crustacean prey. However, we found this specimen consuming a ctenophore. Other deep-sea undescribed physonects with close morphological affinity to our species (L and Zigzag) have been observed consuming fish and squid prey (Choy et al. 2017), thus it is possible that they are specialized in capturing and digesting soft-bodied prey more generally. *Resomia dunni* was predicted to be a generalist (consumer of all types of prey except gelatinous taxa), which is consistent with the copepod prey we found in its gut contents. *Forskalia* species have been observed to consume various crustaceans, molluscs, worms and fish (Purcell 1981a). Morphology predicts *Forskalia* species to be large crustacean specialists. We found three midwater *Forskalia* specimens with copepod prey in the guts, one of them also had consumed a sergestid shrimp. These results are fully congruent with those derived

from visual methods, and partly congruent with the morphological predictions. *Lychnagalma utricularia* is unique among the physonects for bearing a medusa-shaped floating vesicle at the end of their large, coiled tentilla (Damian-Serrano et al. 2021b). They have been observed through ROVs consuming sergestid shrimp. We found two specimens both with sergestid shrimp prey, yet one of them was also digesting a euphausiid (SM-Figure 1). This is consistent with their large-crustacean specialization (Fig. 2, Fig. 5). *Halistemma rubrum* tentilla closely resemble those of *Forskalia*, and thus they are also predicted to be large-crustacean specialists (Damian-Serrano et al. 2021b). This prediction is congruent with our identification of a lophogastrid in the gut contents (Fig. 4).

Nanomia spp. — These are among the most common siphonophores in both Atlantic and Pacific waters, both in epipelagic and midwater environments. We have observed that epipelagic *Nanomia* tend to have smaller tentilla than their mesopelagic counterparts, which may account for their specialization on smaller crustaceans (such as copepods) instead of larger crustaceans (such as krill). Midwater ROV observations of deep-dwelling *Nanomia* have predominantly reported interactions with krill prey, as well as with the occasional chaetognath or sergestid shrimp (Choy et al. 2017). We identified one specimen of mesopelagic *Nanomia* with krill and stomatopod DNA in its gut contents, in agreement with its large-crustacean specialist characterization (Fig. 5). Epipelagic *Nanomia* might not be as specialized on large crustacean prey, since the literature reports a combination of copepod, decapod, mysid, and chaetognath prey (Purcell, 1981a). In the North Pacific Ocean, our metabarcoding identified copepod prey in an epipelagic *Nanomia* off California, a hyperiid amphipod prey in an epipelagic *Nanomia* off Hawaii (SM-Figure 1). The hyperiid amphipod could have been a commensal or parasite on the *Nanomia* instead of prey, though this is unlikely since only the gastrozooids were dissected while amphipods tend to colonize the nectophores or bracts. In the North Atlantic Ocean, we sampled 14 specimens of epipelagic *Nanomia*, seven of which contained copepod prey (Fig. 2). Upon visual inspection of

the sampled gastrozooids we could identify *Temora*, *Centropages*, and *Acartia* copepods, the most abundant genera in the plankton sample, whose identity was also validated by the metabarcoding results. The corresponding environmental plankton samples showed that these waters were dominated by cladocerans, and thus these *Nanomia* were positively selecting for copepod prey and selecting against cladoceran prey (not detected in the guts). The exclusion of the overabundant cladocerans from the diet of Atlantic *Nanomia* suggests that their specialization could be copepod-specific.

Calycophorans — These siphonophores are characterized by their lack of a pneumatophore (gas-filled apical vesicle) and their structurally-homogeneous tentilla (Damian-Serrano et al. 2021b). However, these tentilla present a great variation in nematocyst number and size, which may translate into dietary differences (Damian-Serrano et al. 2021a). We provided insights into the diets of two highly abundant deep-sea calycophorans, *Lensia conoidea* and *Chuniphyes multidentata*, which morphology predicted as small-crustacean specialists. Both sequenced specimens contained copepod DNA, supporting these predictions (Fig. 5). Gelatinous prey has been reported for *Desmophyes annectens* from ROV observations, however we found only copepod prey sequences. We found gelatinous prey in *Diphyes dispar* (salp prey), *Muggiaea atlantica* (larvacean), and *Sphaeronectes christiansonae* (nausithoid medusa). The latter constitutes the first record of *S. christiansonae* feeding. While these medusae can be very small, the minute size of this siphonophore may render this interaction dubious. The far more common epipelagic *Sphaeronectes* species, *S. koellikeri*, appears to be a copepod specialist according to visual gut content analysis (Purcell 1981a). We sequenced the gut contents of two specimens of this species, one of them indeed was consuming a copepod, yet the other was consuming a crab larva. The latter constitutes a novel prey type for this species, yet still within the expected range of a small-crustacean specialist. Another validated expectation occurred with *Sulculeolaria chuni,*

a visually-assessed copepod specialist in Purcell (1981a), for which we detected copepod prey in an Atlantic specimen.

Vogtia is the closest relative to *Hippopodius*, the only siphonophore known to be an ostracod specialist (Purcell 1981a). Like many other hard-to-access mesopelagic taxa, the diet of *Vogtia* has remained unknown, though tentillum morphology predicted them to be generalists (Damian-Serrano et al. 2021b). Pugh (1986) found spatial correlations between ostracods and *Vogtia* species, and even mentions a *Vogtia* sp. specimen which had the exoskeleton of an ostracod in its gut contents. Our DNA metabarcoding on *Vogtia serrata* has revealed one specimen feeding on an ostracod (with high selectivity), and a specimen feeding on a sergestid shrimp and a bivalve. These results are consistent with the generalist morphological prediction, and congruent with the single visual finding of an ostracod in a congener from Pugh (1986). The presence in the gut contents of one of our specimens of an ostracod and a bivalve (likely a pediveliger larva), which has a very similar shape to an ostracod (with two hard valves), indicates phylogenetic conservatism of prey traits within Hippopodiidae.

Comparisons with visual methods

We report the first insights into the diets of nine siphonophore species and reveal 29 novel predator-prey interactions (Fig. 2, Fig. 5). When comparing our metabarcoding findings with the published visual observations from gut content inspections and submersible dives, we found five interactions congruent with ROV observations, and eight interactions (six of them involving copepods) congruent with visual gut content inspections of SCUBA-collected colonies (Fig. 5).

The published records on the diets of siphonophores appear to differ in prey-type composition between epi- and deep-pelagic habitats (Hetherington et al. In review). However, Hetherington et al. (in review) hypothesized that the different methodological limitations inherent to each visual method (small prey underestimated by submersibles, soft-bodied prey

underestimated by gut content inspections) may be responsible for such differences. Our approach has detected prey types, such as larvaceans, ctenophores, bivalves, and ostracods previously missed by visual methods. The gelatinous animals (i.e. ctenophores, medusae, salps) identified by submersibles as prey of deep-pelagic siphonophores were found present in the gut contents of several deep species (*Apolemia* sp., *B. lata,* undescribed physonect L, and *S. christiansonae*), supporting the validity of these observations. However, the gelatinous prey recorded by submersibles in prayids such as *Praya dubia* and *D. annectens* (Choy et al., 2017, Fig. 5) were not recovered in our prayid samples, suggesting that either our sample sizes were not large enough, or that ROVs had observed accidental entanglement of jellies on their tentacle nets which did not end in ingestion. In addition, we found several small crustaceans in the gut contents of epipelagic species (*Forskalia* sp., *Nanomia* sp., *S. koellikeri, S. chuni,* and *D. dispar*) in agreement with visual gut contents observations in shallow habitats. On the other hand, we also found gelatinous and soft-bodied invertebrate prey in shallow-dwelling species (*P. physalis, D. dispar,* and *M. atlantica*); as well as small-bodied animals among the prey deep-pelagic species (*Apolemia* spp., *Bargmannia* spp., *R. dunni, V. serrata, D. annectens, C. multidentata,* and *L. conoidea*) (Fig. 2). Copepods and ctenophores were the most frequent prey among bathypelagic siphonophores, while other crustaceans (such as ostracods, decapods, and krill) appeared as prey more frequently among the mesopelagic taxa. While these findings are consistent with the hypothesis that small prey is underestimated in submersible observations and rapidly-digested, soft-bodied prey is underestimated by gut content inspections, our sample sizes are insufficient to determine whether the relative contribution of these prey differs between habitats.

DNA metabarcoding was able to detect prey both small and large, gelatinous and hard-bodied, for both deep and shallow-dwelling species. These results show that the trophic roles of siphonophores in epi- and deep-pelagic food webs could be more similar than previously-published records may indicate, due to the biases brought by the different diet-assessment

methods applied in each habitat. Vertical migration is an important driver of pelagic food web structure (Sutton 2013, Kelly et al. 2019). We found copepods, decapods, and euphausiids in the gut contents of both meso- and epipelagic siphonophores. These prey taxa are well-known vertical migrators (Longhurst 1976, Hopkins et al. 1994, Cohen & Forward 2009), suggesting that there might be some vertical trophic connectivity between these habitats as prey migrates between them. In addition, a few siphonophore species (including *V. serrata* and *L. conoidea* in this study) are also known diel vertical migrators (Pugh 1984), but their patterns of feeding with depth remain unknown. Finally, our selectivity estimates (for four epipelagic and two mesopelagic species) indicate that siphonophores may play a similar role as selective, specialized predators across all depths in the water column.

Comparisons with prey field

We examined 8 preyfield samples that corresponded to the colocalized ambient prey of 15 out of 47 specimens (some trawls correspond to more than one sampled specimen). The epipelagic plankton samples from Bermuda (colocalized with the *P. physalis* specimens) were dominated by copepods, followed by decapod larvae and chaetognaths. While fish larvae were scarce in these samples, they were still far more abundant than in any other sampled location. The Atlantic epipelagic plankton samples (colocalized with the *S. chuni* and Atlantic shallow *Nanomia* specimens) were dominated by cladocerans, followed by copepods, larvaceans and salps. The Pacific epipelagic plankton sample from California (colocalized with the *D. dispar* specimens) was also dominated by copepods, followed by cladocerans and larvaceans. The quantified midwater tucker trawl from California (colocalized with *V. serrata* specimen D1137-D8 and *Forskalia* sp. Specimen D1137-D9) was also dominated by copepods (albeit larger species), followed by euphausiids (both adult and larval), chaetognaths, and ostracods.

We found both positive and negative selectivity when comparing identified siphonophore prey to quantified co-localized prey fields. We found strong negative (<-0.5) selectivity for

copepods in *P. physalis* specimens and in one specimen of *V. serrata*. However, in 11 specimens from 4 species (out of the 6 species that were quantitatively assessed), we found strong positive selectivity (>0.5) for a specific prey type (SM-Figure 1). These cases include: selectivity for fish in *P. physalis*; selectivity for copepods in *S. chuni*, and Atlantic *Nanomia* sp., selectivity for ostracods in *V. serrata*, and selectivity for salps in *D. dispar* (Fig. 4).

Epipelagic siphonophores are known to be highly selective and specialized carnivores (Purcell 1981a, Purcell & Mills 1988, Mills 1995, Damian-Serrano et al. 2021a). ROV observations have revealed that some deep-sea siphonophores are also highly specialized (Choy et al. 2017). However, the lack of paired diet and planktonic community samples has limited an assessment of their feeding selectivity. For both the shallow- and deep-dwelling siphonophore species assessed here, we found their prey belonged to the less-abundant components of the co-localized planktonic community, demonstrating high prey-type selectivity. However, the selectivity index values presented in this study should be interpreted with care, since the prey field data is quantitative (abundance-based) but the gut content values are only binary at the specimen level, and frequency-based at the species level. Overall, crustaceans (especially copepods) were identified as the most frequent prey type among siphonophore diets. Copepods are typically the most abundant prey type in planktonic communities, thus being able to feed on them is likely an advantageous strategy for any planktivorous predator (Turner 2004). Fish prey were detected only in the Portuguese man-o-war samples, in agreement with published observations of man-o-war feeding.

Our findings are congruent with the idea that siphonophores span multiple trophic positions, consuming prey across low (salps, larvaceans, copepods, ostracods) and high (fish, ctenophores, medusae) trophic levels. We found larvaceans and salps as prey of shallow- and deep-dwelling siphonophores. These thaliaceans have an important role in the biological carbon pump, sequestering carbon from phytoplanktonic producers into the deep sea by means of fecal

matter production and carcass depositions (Robison et al. 2005, Luo et al. 2020). The role of predation on gelatinous herbivores is often underestimated in oceanic food-web models, or primarily attributed to vertebrate predators (Henschke et al. 2016). Our results show that some siphonophores like *Apolemia* sp., *A. lanosa*, *M. atlantica*, and *D. dispar* may play an important mid-trophic role incorporating this gelatinous herbivore productivity into the food web, and providing an alternative avenue to transfer carbon into the deep sea.

Comparisons with morphology predictions

Comparing our metabarcoding findings with the morphology-based predictions from Damian-Serrano et al. (2021b), we found support for 10 of the 16 predicted interactions between siphonophores and prey. Among the physonects, our results supported the predictions of *B. elongata* eating krill and ostracods, *R. dunni* eating copepods, *Forskalia* sp. eating decapods, and *H. rubrum* eating lophogastrids. Among the calycophorans, we found support for the predictions of *V. serrata* eating decapods, ostracods, and molluscs; also *C. multidentata* and *L. conoidea* eating copepods. Among the species studied there were 70 predicted interactions that were not found among the metabarcoding results (Fig. 5). Out of the 10 taxa with both morphology-based predictions and metabarcoding results, six had all prey congruent with the predictions, three had all prey incongruent with the predictions, and *Forskalia* sp. presented both cases.

Food-web structure is determined largely by community composition and its patterns in time and space, as the organismal assemblages determine what predators are present and what prey is available to them (Gotelli & Graves 1996, Ciannelli et al. 2005, Cohen et al. 2012). However, organismal traits constrain which predators can eat which prey (Laigle et al. 2018, Maureaud et al. 2020). The most commonly-studied trait to predict oceanic food web structure has been size (Ward et al. 2012, Zhang et al. 2014). This is due to the importance of gape size in most predators (i.e. fish, squids, crustaceans etc.) with singular and rigid buccal openings (Scharf et al. 2000; Costa 2019). Siphonophores differ from most predators by having many

gastrozooid mouths along their length, all capable of stretching out significantly (Pages & Madin 2010) to ingest prey, sometimes utilizing multiple zooids to wrap around large prey (Hardy 1956). While prey size is still an important constraint for siphonophore-prey interactions (Purcell 1984b), siphonophore size is far less relevant. Moreover, some studies have found that phylogenetically-conserved predator traits other than size may also be important predictors of food web structure (Gilljam et al. 2011, Jacob et al., 2011). Damian-Serrano et al. (2021a) found that diet is a strong predictor of both extant and ancestral siphonophore tentilla morphology, as well as of its evolutionary dynamics. Damian-Serrano et al. (2021b) used these relationships in reverse to predict the diets of understudied siphonophore species based on the morphology of their tentilla and nematocysts. We were able to test these predictions for ten species and found that most of the prey items found were congruent with these predictions, indicating that tentilla morphology is a strong predictor of siphonophore diets. This finding suggests that at least some components of the open-ocean food web are structured by variation in complex morphological traits exclusive to specific predator groups.

Siphonophores are hypothesized to easily evolve between feeding specializations and into a generalist diet due to their modular body plan and their functionally-specialized tentilla (Damian-Serrano et al. 2021a). Our results show that closely-related species such as those within the genera *Bargmannia, Apolemia*, and *Nanomia* may have evolved distinct feeding specializations. These results are congruent with the conclusions from Damian-Serrano et al. (2021a), further indicating that siphonophore dietary evolution can drive rapid shifts even within the same genus. Moreover, we find that *Apolemia* sp., as well as *V. serrata*, could be generalists feeding on a variety of crustacean and soft-bodied prey. These results suggest that a generalist diet may have evolved not just three but up to five times independently, thus reinforcing the conclusions from Damian-Serrano et al. (2021a) on the evolution of feeding guilds.

Methodological considerations

While DNA-based tools can detect prey unrecognized by visual methods, they are not free of shortcomings. Since all life stages of an animal have the same genetic signature, metabarcoding tools are unable to distinguish between larval, juvenile, or adult prey. These ontogenetic stages can have vastly different ecological implications and pose different challenges during prey capture. In addition, the application of metabarcoding to predator diets is usually not quantitative, since too many sources of variation may lead to differences in read abundance. For example, different animal clades have different sizes, cell densities (due to variable acellular mesoglea content), digestion rates, number of copies of the target gene, or primer affinities during the PCR (Deagle & Tollit 2007, Troedsson et al. 2009, Valentini et al. 2009). Due to the difficulties inherent to locating and sampling the species examined in this study, frequency-based quantitative comparisons were not possible for most species either. In addition, the sample size limitations of this study may have biased the results towards higher apparent specialization, and may have missed some important components of the diets of some target species. This caveat is also common in submersible observation data and limits the reliability of comparisons across these methods.

Siphonophores differ from other consumers in several ways which impose further limitations to the value of gut content metabarcoding. The most important aspect is their feeding mode and feeding rate, especially as deep-sea ambush predators, which typically consume one prey at a time and do not get a chance to capture another until far after the former has been digested (Mackie et al. 1988). Therefore, most siphonophores are found with empty guts or digesting one or few prey items at a time. Thus the sample size required for frequency-based analyses is much higher than for other consumers which feed more frequently. Our prey frequency results (Fig. 2) are consistent with this idea. Moreover, except for a couple species such as *Rhizophysa* and *Rosacea* which are diurnal feeders (Purcell 1981a), most species also feed during the night. In the open ocean, diel vertical migration drastically changes the prey field

composition for siphonophores at night (Sutton 2013). Given the fieldwork limitations in this study, we were only able to collect siphonophore gut contents during the day, thus likely biasing their diet towards their diurnal prey captures. Moreover, metabarcoding can only ascertain the taxon of the prey and not the life stage, thus being unable to distinguish between small larval and large adult prey. Finally, secondary predation (the prey of the prey) cannot be empirically distinguished from direct predation, and thus we must rely on natural-history based assumptions.

Conclusions

This study uses DNA metabarcoding technology to investigate the diets of a diverse range of siphonophores. We identified 55 unique prey items in the gut contents of 24 siphonophore species, the majority of which were crustaceans (most of which were copepods), in addition to fishes, molluscs, and gelatinous species (Figs. 2-4). Our results expand the existing knowledge on siphonophore diets, detecting prey types previously missed by visual methods, and providing insights into the diets of several understudied siphonophore species. We show that whole gastrozooids can be utilized for DNA metabarcoding of diets without need for further dissection or the use of predator-blocking primers. We identified representatives from diverse animals (Fig. 3, SM-Figures 6-12), which demonstrates the phylogenetic range of taxa that can be amplified with our primer pairs. By comparing the taxonomic composition of the gut contents to that of the environmental planktonic community, we find support for the idea that most of the examined siphonophore species are specialized on distinct components of zooplankton and micronekton communities (Fig. 4). Many of the prey types found in both shallow and deep-dwelling species match published records based on visual methods, but some prey types appear underrepresented by those methods. Moreover, we find that many of the tentillum morphology-based dietary predictions for these species were supported by the metabarcoding results (Fig. 5).

Overall, we provide novel insights into the ecology and natural history of several siphonophore species, revealing that siphonophores across all depths are specialized and

selective predators which have diversified their feeding habits to consume fish, crustaceans, gelatinous predators, gelatinous filter-feeders, meroplanktonic larvae, and other pelagic invertebrates. Our results reveal a significant involvement of deep- and shallow-dwelling siphonophores in the open-ocean 'jelly web', highlight suspected biases from visual methods, and support the hypothesized value of tentilla morphology to predict their diets. This study also demonstrates the suitability and effectiveness of DNA metabarcoding to identify the prey consumed by gelatinous predators.

Materials and Methods

Siphonophore collections — In order to sample a representative set of taxa across the siphonophore phylogeny, we targeted a set of 41 species (aiming for 10 specimens per species) including cystonects, apolemiids, pyrostephids, euphysonects, and calycophorans from shallow and deep waters (Fig. 2). Most species were sampled from the Offshore California Current Ecosystem (OCCE) except for the Portuguese man-o-war *P. physalis*, which was collected off Bermuda in the Sargasso Sea; *S. chuni* and some *Nanomia* spp. (labeled as "Atlantic") which were collected off Rhode Island in the Block Island sound; *Forskalia* sp. M123-SS8 and shallow *Nanomia* sp. KiloMoana2018-BW7-4 which were collected off the coast of Hawaii. While all the *Nanomia* populations sampled in this study have been referred to as *N. bijuga*, we suspect that there may be undescribed cryptic *Nanomia* species among the specimens sampled based on the disparate tentillum morphologies observed (pers. obs.). Therefore, we decided to have them labeled at the genus level. One *Nanomia* specimen (KiloMoana2018−BW7−4) was collected off the coast of Kona, HI. The pleustonic (surface floating) *Physalia physalis* samples were collected manually using a bucket from a small boat. Species found between the 0-20m deep were collected using blue water diving techniques following the guidelines in Haddock & Heine (2005). Species from 200-4000m were collected using ROVs. All animals were collected live and brought back to

the ship (or field station in Bermuda for *P. physalis*) for dissection (Fig. 1). Live colonies were photographed (sometimes recorded on video), and zooids of diagnostic value (nectophores, bracts, tentacles) were dissected, fixed in 4% formalin, and stored as vouchers at the Yale Peabody Museum of Natural History.

Gut content metabarcoding — Shortly after collection of the live specimens, we dissected and pooled several gastrozooids, prioritizing those with visible gut contents, in addition to any visible egested food pellets at the bottom of the sampling container. Samples were frozen at -80°C until DNA extraction. Further details on the DNA extraction, quality control, PCR, amplicon purification, and amplicon pooling are fully described in the online protocol (dx.doi.org/10.17504/protocols.io.bd8ci9sw). All molecular bench work was carried out at the Yale DNA Analysis Facility. We used a set of six primer pairs that amplify six regions within the 18S gene (and part of the ITS1) named after their expected amplicon length ('134', '152', '166', '179', '261', and '272'). The primers were designed using Geneious v.x.x.x. (Kearse et al. 2012), seeking short (>300bp) amplicon products with a high chance of remaining uncleaved after digestion in the gastrozooid, flanked by priming sites conserved (to a maximum mismatch of 3bp) across metazoans. The search for conserved priming sites was conducted on an alignment of 18S genes from 975 species across all metazoan phyla downloaded from GenBank. The primer search was optimized to only retrieve primer pairs with compatible annealing temperatures and without problematic dimerization and hairpin temperatures. Primer sequences and properties can be found in Table T1 in Damian-Serrano (2020). Amplicon pools were sequenced using Illumina MiSeq 250bp paired-end technology (except samples in run 0 which was sequenced using MiSeq 150bp) at the Yale Center for Genomic Analysis.

Prey reference database — In order to enhance the accuracy of the taxonomic assignments of reads, we also built an 18S gene barcoding database. To do this, we collected 60 specimens of 30 species of zooplankton and micronekton from the OCCE using a Tucker trawl.

We targeted plausible prey species from motile open-ocean taxa that cohabitate with siphonophores and are underrepresented in SILVA databases, including fishes, crustaceans, jellyfishes, urochordates, chaetognaths, polychaetes, and mollusks. Specimens were photographed live, tissue was sampled and frozen, and the rest of the animal was fixed in formalin as a voucher to be identified and preserved at the Yale Peabody Museum of Natural History. DNA extraction, quality control, PCR, and amplicon cleanup was carried out in a similar fashion as the metabarcoding protocol in Damian-Serrano (2020), except that only one PCR program (https://dx.doi.org/10.17504/protocols.io.bd8ci9sw, Table T5A), and only one pair of primers were used (166F and 134R), spanning the full extent of the sequence containing all barcode regions used in the gut content metabarcoding (~1800bp). Purified amplicons were sent in plates with the forward and reverse primer separately for Sanger sequencing from both ends at the Yale DNA Analysis Facility. These sequences were then assembled and trimmed at a 95% quality cutoff in Geneious and concatenated with the latest SILVA database (SILVA_138_SSURef_NR99 pruned to remove bacterial sequences) downloaded on February 23, 2021 to generate our custom-built database.

Bioinformatic pipeline — Amplicon libraries were demultiplexed by primer sequence using custom bash code. Primer sequences were removed using *cutadapt* (Martin 2011). The forward and reverse reads were matched and repaired using *bbtools* (Bushnell et al. 2017), then denoised and de-replicated using the DADA2 (Callahan et al. 2016) plugin in QIIME2 (Bolyen et al. 2019) with a truncation quality threshold of 28. We *de novo* clustered the unique features into OTUs using the VSEARCH (Rognes et al. 2016) plugin in QIIME2 with a similarity threshold of 95%. Using QIIME2, we computed sample composition and diversity metrics and aligned the feature sequences with MAFFT (Katoh et al. 2009) to build a phylogenetic tree with Fasttree (Price et al. 2009). To reduce computational load, only the top 100 most abundant features among the clustered OTUs were selected for taxonomic assignment. Taxonomic identifications were

assigned using the assignment software METAXA2 (Bengtsson-Palme et al. 2015) with a 70% reliability cutoff, comparing the sequences against the standard GenBank reference library, the SILVA123.1 reference library (Quast et al. 2012), and our custom-built library (based on SILVA138). All bioinformatics analyses were carried out in the Yale High Performance Computing Cluster. The taxonomic assignments and read count data were merged, then parsed to match the sample of origin and the DNA sequence they derived from. Sequence post-processing scripts can be found in the GitHub repository (https://github.com/dunnlab/siphweb_metabarcoding).

Assignment interpretation — Taxonomic assignments were manually inspected and annotated with the interpreted consensus taxon and interpreted source (predator, prey, secondary predation, parasite, environmental eukaryote, unrecognizable sequence, contamination, or cross contamination). A combination of annotation database consensus, barcode region consensus, number of reads, manual BLAST checks, and natural history informed priors were used to assign these interpretations. Amplification experiments on negative controls indicated that the human, mite, and insect contaminants originated from specimen manipulation in the field and not from the lab bench. Cross-contamination at the lab bench was suspected for some samples in runs 0 and 5 due to simultaneous DNA extractions of reference prey samples. Reads suspected of cross-contamination (assigned to taxa present in the potential sources of contamination, present across multiple samples in the same run with very low read abundances) were conservatively labelled as such. Crustacean, gastropod, and larvacean sequences in *Physalia* samples were interpreted as secondary predation (prey of their fish prey) given our knowledge on the prey-capture limitations of these animals and the feeding habits of their fish prey. When all barcode regions except ‘152’ indicate mysid prey but ‘152’ identifies a similar number of reads as stomatopod prey, we interpret those reads as mysid prey. Assignments of shark identities by barcode region ‘152’ in one of the *Physalia* samples (extraction 169) were identified as ray-finned fish prey using BLAST searches and interpreted as such, in agreement with the other barcode regions.

Assignments of decapod crustacean identities by barcode region ‘152’ (in extractions 111, 218, and 225) were interpreted as euphausiid prey in agreement with the assignments on the rest of the barcode regions. The taxonomic composition of the samples was analyzed and visualized in the R programming environment. Scripts and data available in our GitHub repository.

Prey field characterization — In order to compare the observed diet to the environmental abundances of potential prey taxa, we collected zooplankton and micronekton samples on the same day and station location as the relevant siphonophore gut content samples. The plankton samples paired with epipelagic siphonophore specimens were collected using a weighted hand-held plankton net (ring diameter of 1m for the Bermuda samples, 0.5m for the OCCE and Block Island sound samples, mesh size of 250µm) towed for ~10min at a few meters depth at a speed of ~1kt. Paired with the ROV-collected mesopelagic siphonophore specimens, we collected zooplankton and micronekton samples using a Tucker trawl (frame area: $2m^2$, mesh size: 500µm) towed for ~2h between 900m and the surface at night. Environmental community samples were visually examined live to collect specimens to sequence for the 18S reference library and other purposes, which were annotated as removed. Samples were concentrated using metal sieves and fixed in 4% formalin. Back in the Yale Peabody Museum of Natural History, these samples were visually identified and quantified from a splitter aliquot. Identifications were carried out to the lowest taxonomic level as well as to a broad group level (e.g., copepods, decapods, krill, fish, hydromedusae, chaetognaths, polychaetes etc.). A few individual specimens were removed from the haul before preservation to serve other scientific goals during fieldwork, and therefore these samples may be imperfect representations of the community. In order to estimate how selective siphonophore species are for different prey types in the environment, we calculated Strauss (1979) Linear Index (LI) at the broad taxonomic group level.

$$LI = r_i - p_i$$

We used this index to capture the difference between the fraction of each prey type in the environment (p_i) and the observed frequencies of prey types in the gut contents (r_i).

Comparisons to published sources — We aimed to compare and expand previous predation results from submersible observations and visual gut content inspections with the new results of DNA metabarcoding of gut contents. Therefore, we used the dietary data compiled in Damian-Serrano et al. (2021a) from 11 published sources divided into those that used gut content inspections and those that used human- and remotely-operated submersible observations. Many of the submersible observations correspond to ROV observations carried out in the Offshore California Current Ecosystem, spatially overlapping with the location where the majority of our metabarcoding samples were collected. Salps, ctenophores, and medusae were merged into a gelatinous prey type for comparative purposes. Published records for *Apolemia uvaria* were considered equivalent to *Apolemia* sp. for genus level comparisons. Records of all *Forskalia* species were considered equivalent to *Forskalia* sp. In order to test the morphology-based dietary predictions generated in Damian-Serrano et al. (2021b), we used the Bayesian posterior probabilities for each feeding guild for each species. Small-crustacean guild predictions were mapped to copepod, ostracod, and cladoceran prey. Large-crustacean guild predictions were mapped to decapod, euphausiid, mysid, lophogastrid, stomatopod, and amphipod prey. Generalist guild predictions were mapped to all prey types except gelatinous prey (following the intended distinction with gelatinous specialists used in Damian-Serrano et al. 2021a).

Acknowledgements

We thank Gisella Caccone, Carol Mariani, and T.J. Johnson for the Yale DNA Analysis Facility for their invaluable training and their assistance on this study, as well as the staff of the Yale Center for Genomic Analyses for helping us design the sequencing strategy for this study, and the Yale Center for Research Computing for providing assistance with high-performance computing. We thank Bianca R. Brown for her assistance designing the read processing pipeline

and Johan Bengtsson-Palme for his help troubleshooting our usage of METAXA2. We are grateful to the crews of the R/V Western Flyer and R/V Kilo Moana, the Bermuda Institute of Ocean Sciences, and Jeff Godfrey for making the collection of these samples possible. This research was funded by the Yale Institute of Biospheric Studies through a Doctoral Dissertation Improvement Award to A.D.-S., as well as by NSF-OCE 1829835 (to C.W.D.), OCE-1829805 (to S.H.D.H.), and OCE-1829812 (to C.A.C.).

References

Bardi J, Marques AC. Taxonomic redescription of the Portuguese man-of-war, Physalia physalis (Cnidaria, Hydrozoa, Siphonophorae, Cystonectae) from Brazil. Iheringia. Série Zoologia. 2007;97:425-33.

Bengtsson-Palme J, Hartmann M, Eriksson KM, Pal C, Thorell K, Larsson DG, Nilsson RH. METAXA2: improved identification and taxonomic classification of small and large subunit rRNA in metagenomic data. Molecular ecology resources. 2015 Nov;15(6):1403-14.

Biggs DC. Field studies of fishing, feeding, and digestion in siphonophores. Marine & Freshwater Behaviour & Phy. 1977 Jan 1;4(4):261-74.

Bolyen E, Rideout JR, Dillon MR, Bokulich NA, Abnet CC, Al-Ghalith GA, Alexander H, Alm EJ, Arumugam M, Asnicar F, Bai Y. Reproducible, interactive, scalable and extensible microbiome data science using QIIME 2. Nature biotechnology. 2019 Aug;37(8):852-7.

Bushnell B, Rood J, Singer E. BBMerge–Accurate paired shotgun read merging via overlap. PLoS one. 2017 Oct 26;12(10):e0185056.

Callahan BJ, McMurdie PJ, Rosen MJ, Han AW, Johnson AJ, Holmes SP. DADA2: high-resolution sample inference from Illumina amplicon data. Nature methods. 2016 Jul;13(7):581-3.

Chi X, Dierking J, Hoving HJ, Lüskow F, Denda A, Christiansen B, Sommer U, Hansen T, Javidpour J. Tackling the jelly web: Trophic ecology of gelatinous zooplankton in oceanic food

webs of the eastern tropical Atlantic assessed by stable isotope analysis. Limnology and Oceanography. 2021 Feb;66(2):289-305.

Choy CA, Haddock SH, Robison BH. Deep pelagic food web structure as revealed by in situ feeding observations. Proceedings of the Royal Society B: Biological Sciences. 2017 Dec 6;284(1868):20172116.

Ciannelli L, Hjermann DØ, Lehodey P, Ottersen G, Duffy-Anderson JT, Stenseth NC. Climate forcing, food web structure and community dynamics in pelagic marine ecosystems. Aquatic food webs: an ecosystem approach. Oxford University Press, Oxford. 2005 Apr 7:143-69.

Clarke LJ, Trebilco R, Walters A, Polanowski AM, Deagle BE. DNA-based diet analysis of mesopelagic fish from the southern Kerguelen Axis. Deep Sea Research Part II: Topical Studies in Oceanography. 2020 Apr 1;174.

Cohen JH, Forward Jr RB. Zooplankton diel vertical migration—a review of proximate control. Oceanography and marine biology. 2016 Apr 19:89-122.

Cohen JE, Briand F, Newman CM. Community food webs: data and theory. Springer Science & Business Media; 2012 Dec 6.

Connell SC, O'Rorke R, Jeffs AG, Lavery SD. DNA identification of the phyllosoma diet of *Jasus edwardsii* and *Scyllarus* sp. Z. New Zealand Journal of Marine and Freshwater Research. 2014 Jul 3;48(3):416-29.

Costa GC. Predator size, prey size, and dietary niche breadth relationships in marine predators. Ecology. 2009 Jul;90(7):2014-9.

Damian-Serrano A, Haddock SH, Dunn CW. The evolution of siphonophore tentilla for specialized prey capture in the open ocean. Proceedings of the National Academy of Sciences. 2021a Feb 23;118(8).

Damian-Serrano A, Haddock SH, Dunn CW. The evolutionary history of siphonophore tentilla: Novelties, convergence, and integration. Integrative Organismal Biology. 2021b May 26.

Deagle BE, Tollit DJ. Quantitative analysis of prey DNA in pinniped faeces: potential to estimate diet composition?. Conservation Genetics. 2007 Jun;8(3):743-7.

Falkowski PG, Barber RT, Smetacek V. Biogeochemical controls and feedbacks on ocean primary production. Science. 1998 Jul 10;281(5374):200-6.

Fernández-Álvarez FÁ, Machordom A, García-Jiménez R, Salinas-Zavala CA, Villanueva R. Predatory flying squids are detritivores during their early planktonic life. Scientific Reports. 2018 Feb 21;8(1):1-2.

Gilljam D, Thierry A, Edwards FK, Figueroa D, Ibbotson AT, Jones JI, Lauridsen RB, Petchey OL, Woodward G, Ebenman B. Seeing double:: Size-based and taxonomic views of food web structure. Advances in ecological research. 2011 Jan 1;45:67-133.

Gotelli NJ, Graves GR. Null models in ecology. 1996.

Griffiths D. Prey availability and the food of predators. Ecology. 1975 Aug;56(5):1209-14.

Grossmann MM, Nishikawa J, Lindsay DJ. Diversity and community structure of pelagic cnidarians in the Celebes and Sulu Seas, southeast Asian tropical marginal seas. Deep Sea Research Part I: Oceanographic Research Papers. 2015 Jun 1;100:54-63.

Haddock SH. A golden age of gelata: past and future research on planktonic ctenophores and cnidarians. Hydrobiologia. 2004 Nov;530(1):549-56.

Haddock SH, Heine JN. Scientific blue-water diving La Jolla. CA: California Sea Grant College Program. 2005.

Harbison GR. The gelatinous inhabitants of the ocean interior. Oceanus. 1992;35:18-23.

Hardy SA. The open sea, its natural history, the world of plankton. 1956. No. 574.92 H3.

Harms-Tuohy CA, Schizas NV, Appeldoorn RS. Use of DNA metabarcoding for stomach content analysis in the invasive lionfish Pterois volitans in Puerto Rico. Marine Ecology Progress Series. 2016 Oct 25;558:181-91.

Henschke N, Everett JD, Richardson AJ, Suthers IM. Rethinking the role of salps in the ocean. Trends in Ecology & Evolution. 2016 Sep 1;31(9):720-33.

Hetherington ED, Damian-Serrano A, Haddock SHD, Dunn CW, Choy CA. Moving beyond medusae: Integrating siphonophores into marine food web ecology. *Limnology and Oceanography Letters*. Under review.

Hopkins TL, Flock ME, Gartner Jr JV, Torres JJ. Structure and trophic ecology of a low latitude midwater decapod and mysid assemblage. Marine Ecology Progress Series. 1994 Jun 23:143-56.

Jacob U, Thierry A, Brose U, Arntz WE, Berg S, Brey T, Fetzer I, Jonsson T, Mintenbeck K, Möllmann C, Petchey OL. The role of body size in complex food webs: A cold case. Advances in ecological research. 2011 Jan 1;45:181-223.

Jamieson AJ, Linley TD. Hydrozoans, scyphozoans, larvaceans and ctenophores observed in situ at hadal depths. Journal of Plankton Research. 2021 Jan;43(1):20-32.

Jensen MR, Knudsen SW, Munk P, Thomsen PF, Møller PR. Tracing European eel in the diet of mesopelagic fishes from the Sargasso Sea using DNA from fish stomachs. Marine Biology. 2018 Aug;165(8):1-1.

Katoh K, Asimenos G, Toh H. Multiple alignment of DNA sequences with MAFFT. InBioinformatics for DNA sequence analysis 2009 (pp. 39-64). Humana Press.

Kearse M, Moir R, Wilson A, Stones-Havas S, Cheung M, Sturrock S, Buxton S, Cooper A, Markowitz S, Duran C, Thierer T. Geneious Basic: an integrated and extendable desktop

software platform for the organization and analysis of sequence data. Bioinformatics. 2012 Jun 15;28(12):1647-9.

Kelly TB, Davison PC, Goericke R, Landry MR, Ohman MD, Stukel MR. The importance of mesozooplankton diel vertical migration for sustaining a mesopelagic food web. Frontiers in Marine Science. 2019 Sep 13;6:508.

Laigle I, Aubin I, Digel C, Brose U, Boulangeat I, Gravel D. Species traits as drivers of food web structure. Oikos. 2018 Feb;127(2):316-26.

Leray M, Yang JY, Meyer CP, Mills SC, Agudelo N, Ranwez V, Boehm JT, Machida RJ. A new versatile primer set targeting a short fragment of the mitochondrial COI region for metabarcoding metazoan diversity: application for characterizing coral reef fish gut contents. Frontiers in zoology. 2013 Dec;10(1):1-4.

Longhurst AR. Vertical Migration. The Ecology of the Seas, DH Cushing and JJ Walsh, eds., Philadelphia: University of Pennsylvania Press; 1976.

Luo JY, Condon RH, Stock CA, Duarte CM, Lucas CH, Pitt KA, Cowen RK. Gelatinous zooplankton-mediated carbon flows in the global oceans: a data-driven modeling study. Global Biogeochemical Cycles. 2020 Sep;34(9):e2020GB006704.

Mackie GO, Pugh PR, Purcell JE. Siphonophore biology. Advances in Marine biology. 1988 Jan 1;24:97-262.

Mapstone GM. Global diversity and review of Siphonophorae (Cnidaria: Hydrozoa). PLoS One. 2014 Feb 6;9(2):e87737.

Marques R, Darnaude AM, Crochemore S, Bouvier C, Bonnet D. Molecular approach indicates consumption of jellyfish by commercially important fish species in a coastal Mediterranean lagoon. Marine environmental research. 2019 Dec 1;152:104787.

Martin M. Cutadapt removes adapter sequences from high-throughput sequencing reads. EMBnet. journal. 2011 May 2;17(1):10-2.

Maureaud A, Andersen KH, Zhang L, Lindegren M. Trait-based food web model reveals the underlying mechanisms of biodiversity–ecosystem functioning relationships. Journal of Animal Ecology. 2020 Jun;89(6):1497-510.

McInnes JC, Alderman R, Lea MA, Raymond B, Deagle BE, Phillips RA, Stanworth A, Thompson DR, Catry P, Weimerskirch H, Suazo CG. High occurrence of jellyfish predation by black-browed and Campbell albatross identified by DNA metabarcoding. Molecular Ecology. 2017 Sep;26(18):4831-45.

Mills CE. Medusae, siphonophores, and ctenophores as planktivorous predators in changing global ecosystems. ICES Journal of Marine Science. 1995 Jun 1;52(3-4):575-81.

O'Brien TD. COPEPOD, a global plankton database: A review of the 2007 database contents and new quality control methodology. 2017 https://www.st.nmfs.noaa.gov/copepod/

Pagès F, Madin LP. Siphonophores eat fish larger than their stomachs. Deep Sea Research Part II: Topical Studies in Oceanography. 2010 Dec 1;57(24-26):2248-50.

Price MN, Dehal PS, Arkin AP. FastTree: computing large minimum evolution trees with profiles instead of a distance matrix. Molecular biology and evolution. 2009 Jul 1;26(7):1641-50.

Pugh PR. The diel migrations and distributions within a mesopelagic community in the North East Atlantic. 7. Siphonophores. Progress in Oceanography. 1984 Jan 1;13(3-4):461-89.

Pugh PR. Trophic factors affecting the distribution of siphonophores in the North Atlantic Ocean. UNESCO Technical Papers in Marine Science. 1986;49:230-4.

Purcell JE. Dietary composition and diel feeding patterns of epipelagic siphonophores. Marine Biology. 1981 Nov;65(1):83-90.

Purcell JE. Feeding ecology of *Rhizophysa eysenhardti*, a siphonophore predator of fish larvae. Limnology and Oceanography. 1981 May;26(3):424-32.

Purcell JE. Predation on fish larvae by *Physalia physalis*, the Portuguese man of war. Marine ecology progress series. Oldendorf. 1984a Jan 1;19(1):189-91.

Purcell JE. The functions of nematocysts in prey capture by epipelagic siphonophores (Coelenterata, Hydrozoa). The Biological Bulletin. 1984b Apr;166(2):310-27.

Purcell JE, Mills, CE. The correlation between nematocyst types and diets in pelagic hydrozoa. The biology of nematocysts. 1988:463-85.

Quast C, Pruesse E, Yilmaz P, Gerken J, Schweer T, Yarza P, Peplies J, Glöckner FO. The SILVA ribosomal RNA gene database project: improved data processing and web-based tools. Nucleic acids research. 2012 Nov 27;41(D1):D590-6.

Van der Reis AL, Laroche O, Jeffs AG, Lavery SD. Preliminary analysis of New Zealand scampi (*Metanephrops challengeri*) diet using metabarcoding. PeerJ. 2018 Sep 20;6:e5641.

Robison BH. Deep pelagic biology. Journal of experimental marine biology and ecology. 2004 Mar 31;300(1-2):253-72.

Robison BH, Reisenbichler KR, Sherlock RE. Giant larvacean houses: Rapid carbon transport to the deep sea floor. Science. 2005 Jun 10;308(5728):1609-11.

Rognes T, Flouri T, Nichols B, Quince C, Mahé F. VSEARCH: a versatile open source tool for metagenomics. PeerJ. 2016 Oct 18;4:e2584.

Scharf FS, Juanes F, Rountree RA. Predator size-prey size relationships of marine fish predators: interspecific variation and effects of ontogeny and body size on trophic-niche breadth. Marine Ecology Progress Series. 2000 Dec 8;208:229-48.

Strauss RE. Reliability estimates for Ivlev's electivity index, the forage ratio, and a proposed linear index of food selection. Transactions of the American Fisheries Society. 1979 Jul;108(4):344-52.

Sutton TT. Vertical ecology of the pelagic ocean: classical patterns and new perspectives. Journal of fish biology. 2013 Dec;83(6):1508-27.

Troedsson C, Simonelli P, Nägele V, Nejstgaard JC, Frischer ME. Quantification of copepod gut content by differential length amplification quantitative PCR (dla-qPCR). Marine Biology. 2009 Feb;156(3):253-9.

Turner JT. The importance of small planktonic copepods and their roles in pelagic marine food webs. Zoological studies. 2004 Jan;43(2):255-66.

Valentini A, Miquel C, Nawaz MA, Bellemain EV, Coissac E, Pompanon F, Gielly L, Cruaud C, Nascetti G, Wincker P, Swenson JE. New perspectives in diet analysis based on DNA barcoding and parallel pyrosequencing: the trnL approach. Molecular ecology resources. 2009 Jan;9(1):51-60.

Ward BA, Dutkiewicz S, Jahn O, Follows MJ. A size-structured food-web model for the global ocean. Limnology and Oceanography. 2012 Nov;57(6):1877-91.

Zhang L, Hartvig M, Knudsen K, Andersen KH. Size-based predictions of food web patterns. Theoretical ecology. 2014 Feb;7(1):23-33.

Figures

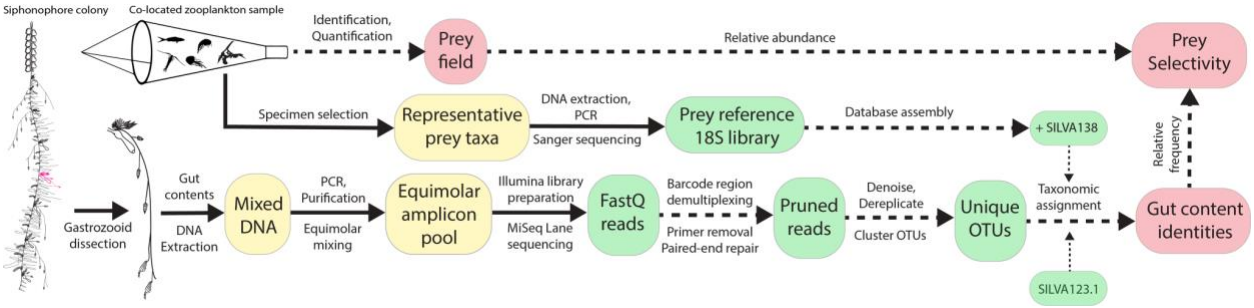

Figure 1. Gut content metabarcoding workflow used in this study. Siphonophore colony illustrated by Freya Goetz. Silhouettes in the plankton net downloaded from phylopic.org. Solid arrows indicate physical material transfer and processing, dashed lines indicate information transfers and processing. Yellow islands indicate elements processed in the laboratory bench, green islands represent bioinformatic datasets processed in the high-performance computing cluster, and red islands represent curated data products.

Species	Vertical habitat	N sampled	N with prey	Literature-based guild	Tentilla-based prediction of guild	Metabarcoding prey	Photo
Physalia physalis	Pleustonic	5	3	Fish		Fish, ctenophore	A
Undescribed physonect ZigZag	Mesopelagic	1	0				
Undescribed physonect L	Bathypelagic	2	1		Fish	Ctenophore	B
Erenna sirena	Bathypelagic	2	0	Fish			
Erenna cornuta	Bathypelagic	1	0				
Stephanomia amphytridis	Bathypelagic	3	0				
Apolemia rubriversa	Mesopelagic	7	2	Gelatinous		Copepod, salp	
Apolemia sp.	Mesopelagic	3	3	Gelatinous		Copepod, mysid, euphausid, ctenophore, larvacean	
Apolemia lanosa	Bathypelagic	3	1		Gelatinous	Copepod	C
Nanomia sp. shallow Pacific	Epipelagic	12	2	Large crustacean		Copepod, amphipod	
Nanomia sp. shallow Atlantic	Epipelagic	14	9			Copepod	
Halistemma rubrum	Epipelagic	1	1		Large crustacean	Lophogastrid	
Nanomia sp. deep	Mesopelagic	3	1	Large crustacean		Euphausid, stomatopod	D
Lychnagalma utricularia	Mesopelagic	4	2	Large crustacean		Decapod, euphausid	E
Resomia ornicephala	Mesopelagic	1	0	Large crustacean			
Craseoa lathetica	Mesopelagic	2	0		Large crustacean		
Lilyopsis fluoracantha	Mesopelagic	1	0		Large crustacean		
Praya dubia	Mesopelagic	2	0	Large crustacean			
Desmophyes annectens	Mesopelagic	1	1			Copepod	F
Bargmannia elongata	Mesopelagic	2	1		Large crustacean	Ostracod, euphausid	
Bargmannia amoena	Bathypelagic	3	2	Large crustacean		Copepod, mysid	
Bargmannia lata	Bathypelagic	3	2		Large crustacean	Copepod, ctenophore	
Marrus claudanielis	Bathypelagic	2	0		Large crustacean		
Forskalia sp.	Epipelagic	3	3	Generalist		Copepod, decapod	
Agalma okenii	Epipelagic	3	0	Generalist			
Frillagalma vityazi	Mesopelagic	3	0		Generalist		
Vogtia serrata	Mesopelagic	3	2		Generalist	Ostracod, decapod, bivalve	G
Resomia dunni	Bathypelagic	3	1		Generalist	Copepod	H
Sulculeolaria chuni	Epipelagic	1	1	Small crustacean		Copepod	
Muggiaea atlantica	Epipelagic	5	1	Small crustacean		Larvacean	
Diphyes dispar	Epipelagic	15	3	Small crustacean		Copepod, euphausid, salp	I
Cordagalma ordinatum	Epipelagic	1	0	Small crustacean			
Sphaeronectes koellikeri	Epipelagic	10	2	Small crustacean		Copepod, decapod	J
Sphaeronectes christiansonae	Mesopelagic	1	1			Scyphomedusa	
Lensia conoidea	Mesopelagic	1	1		Small crustacean	Copepod	
Chuniphyes multidentata	Mesopelagic	5	1		Small crustacean	Copepod	
Gymnopraia lapislazula	Mesopelagic	3	0		Small crustacean		
Kephyes ovata	Mesopelagic	2	0		Small crustacean		
Chuniphyes moserae	Bathypelagic	1	0		Small crustacean		

Figure 2. Summary table of the siphonophore species sampled for this study indicating their

vertical habitat, the number of specimens sampled, the number of specimens with recognizable prey sequences, hypothesized feeding guild based on published feeding records used in Damian-Serrano et al. (2021a), predicted feeding guild from the DAPC analysis in Damian-Serrano et al. (2021b) based on tentilla morphology, and prey found in this study. Photo credits: (A) C.W.D., (B) Schmidt Ocean, (C) MBARI, (D) Reyn Yoshioka, (E) MBARI, (F) Pugh et al. 2020, (G-H) MBARI, (I) Russell Hopcroft , (J) Denis Riek.

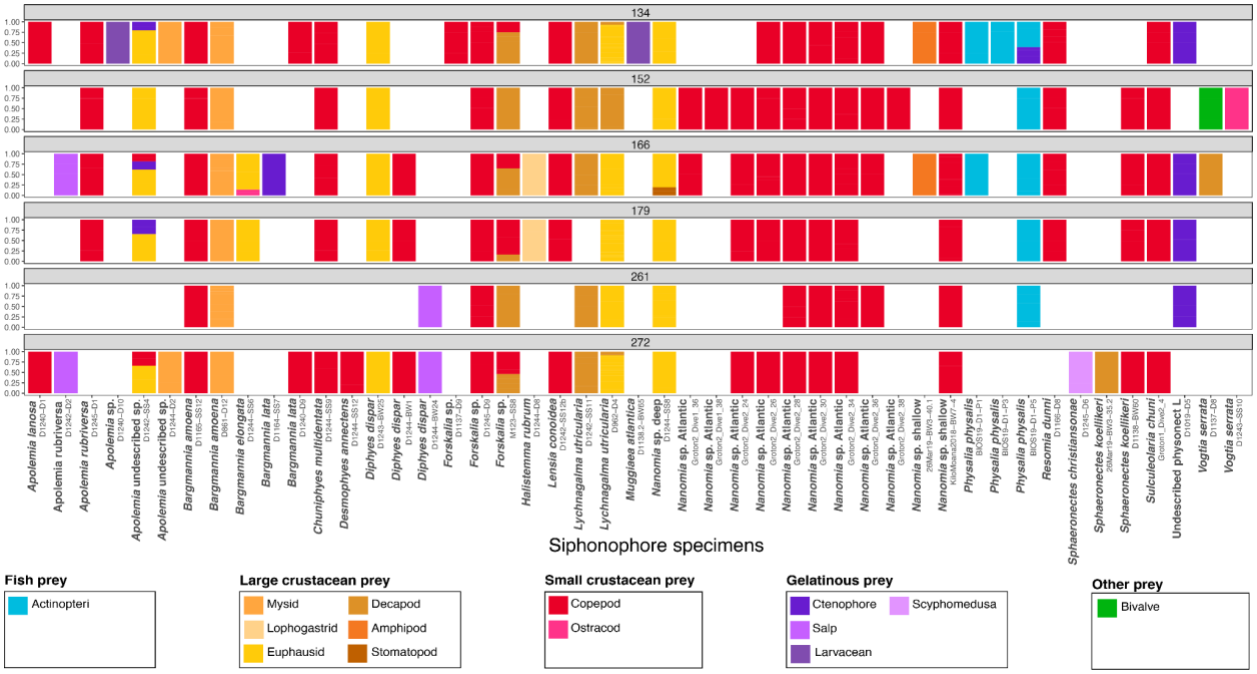

Figure 3. Relative read log-abundance of prey colored by prey taxon for each specimen and barcode.

Figure 4. Species-wise grid with the frequency of the major prey types identified from the metabarcoding data (left) and the average prey-type selectivity estimated in comparison with the local planktonic community composition (right). Gut content cells in white indicate absence, and cells in grey indicate presence in one specimen, or more than one specimen if labeled with a number. Selectivity colors mapped to Strauss' L.I. values. The siphonophore cladogram (left) is a simplified version of the phylogenetic tree published in Damian-Serrano et al. (2021a).

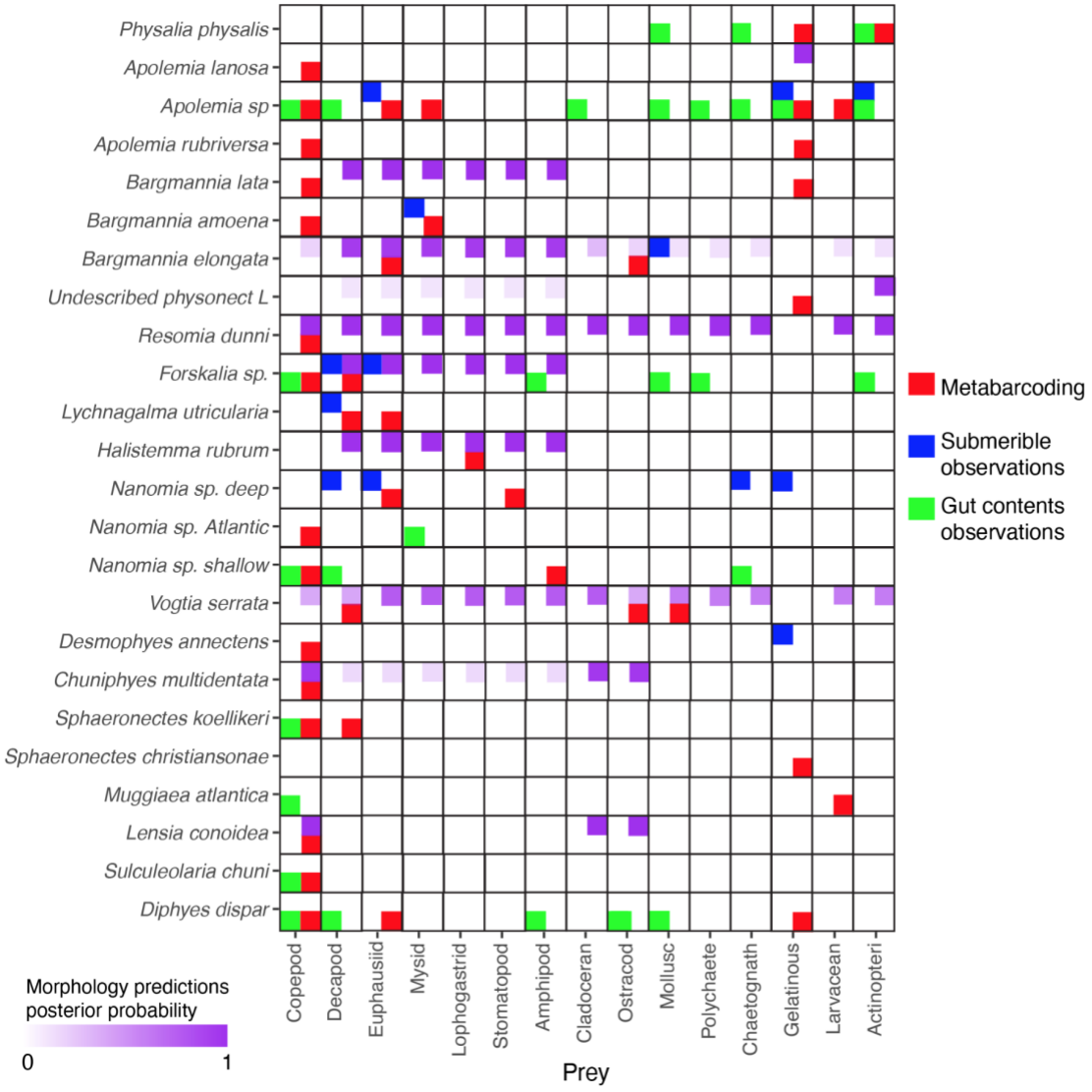

Figure 5. Feeding interactions between siphonophore species and their prey identified by our metabarcoding results (red), published submersible observations (blue), published visual gut content analyses (green), and predicted by the morphology-based DAPC model in Damian-Serrano et al. (2021b).

Supporting Information

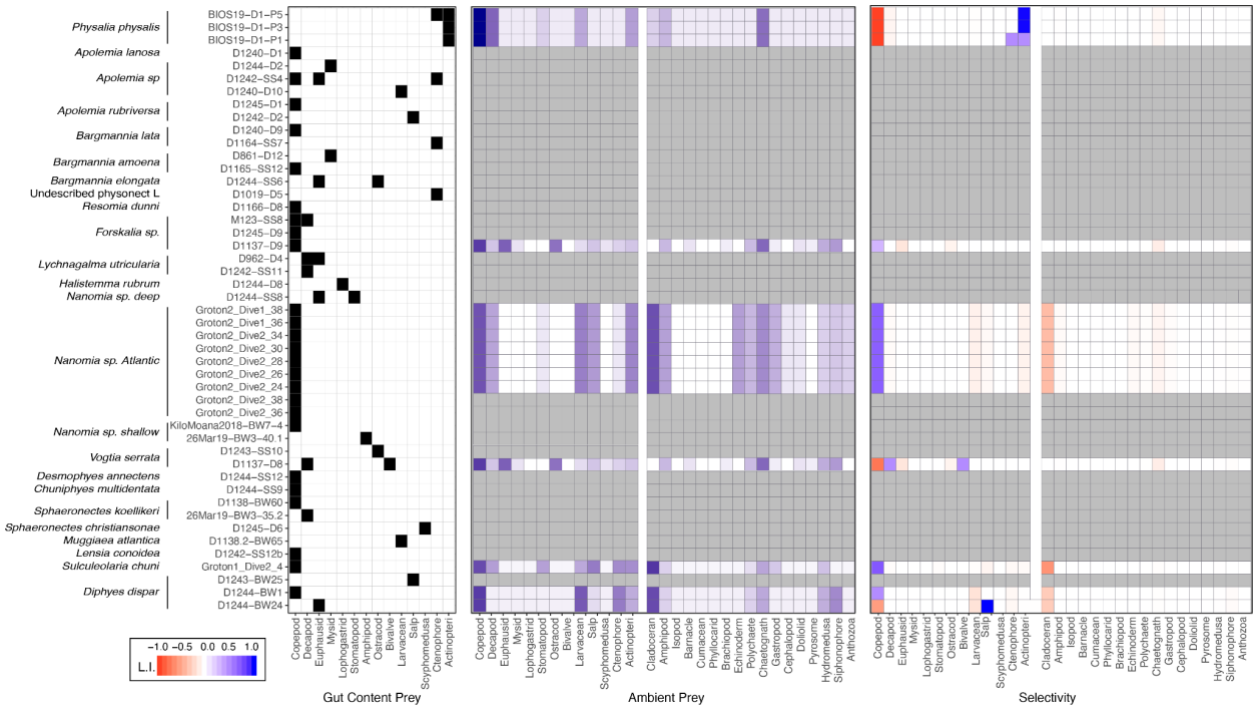

SM-Figure 1. Species-wise grid with the frequency of the major prey types identified from the metabarcoding data (left) and the average prey-type selectivity estimated in comparison with the local planktonic community composition (right). Gut content cells in white indicate absence, and cells in grey indicate presence in one specimen, or more than one specimen if labeled with a number. Selectivity colors mapped to Strauss' L.I. values.

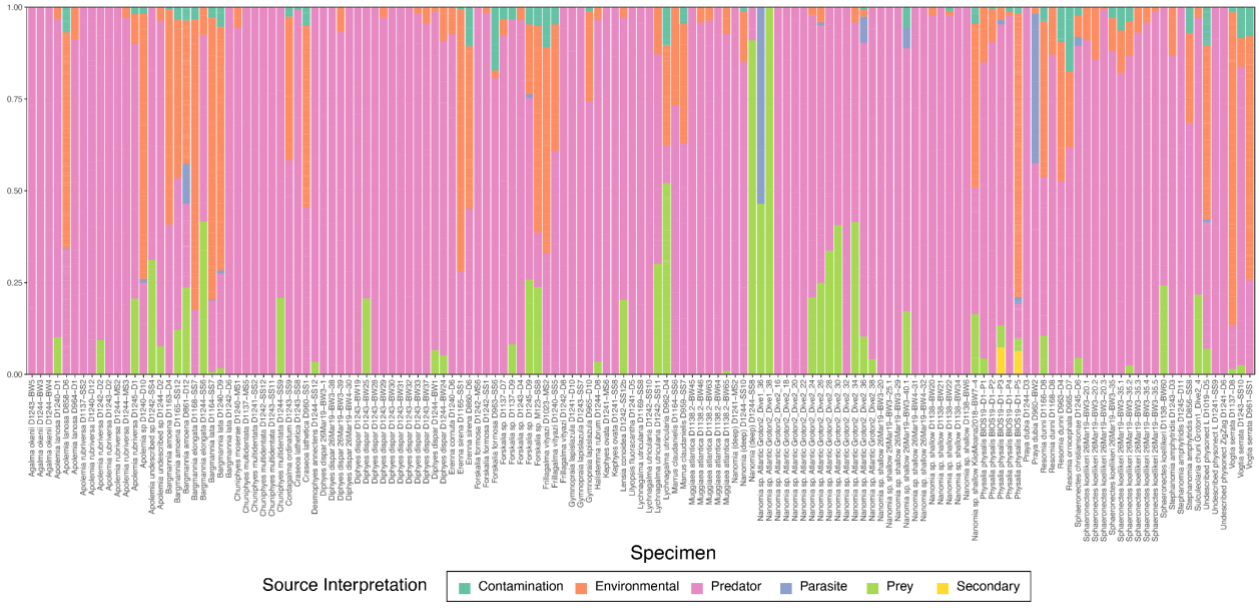

SM-Figure 2. Relative read log-abundance colored by OTU source interpretation for each species.

SM-Figure 3. Relative read log-abundance colored by OTU source interpretation for each species and barcode region.

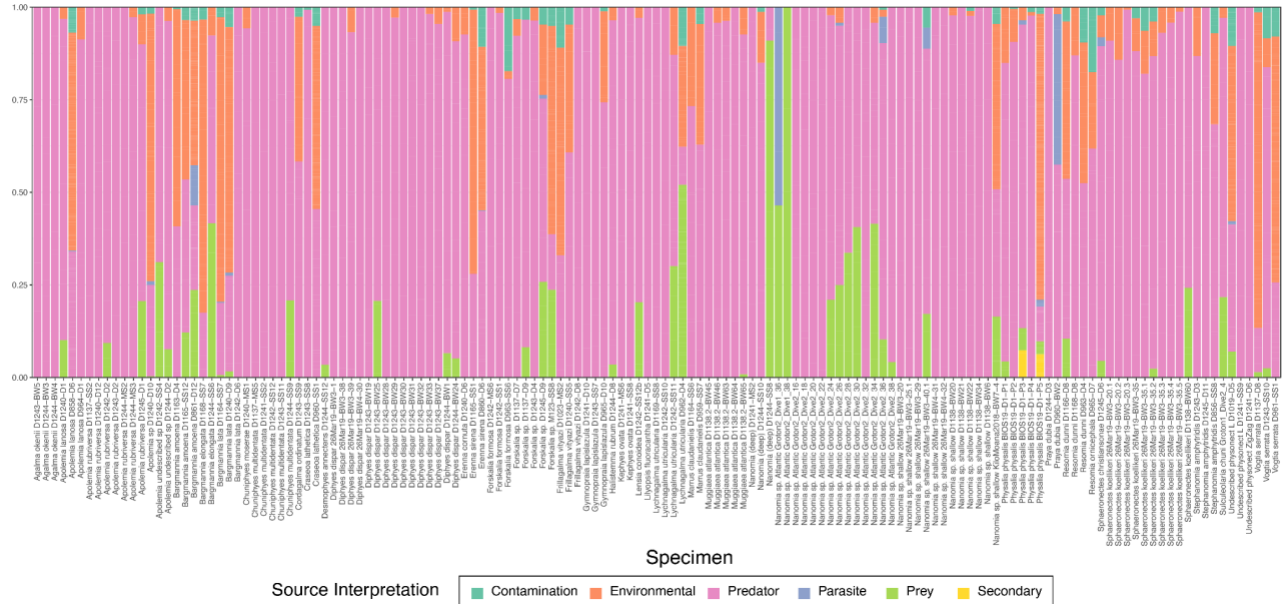

SM-Figure 4. Relative read log-abundance colored by OTU source interpretation for each specimen.

SM-Figure 5. Relative read log-abundance colored by OTU source interpretation for each specimen and barcode region.

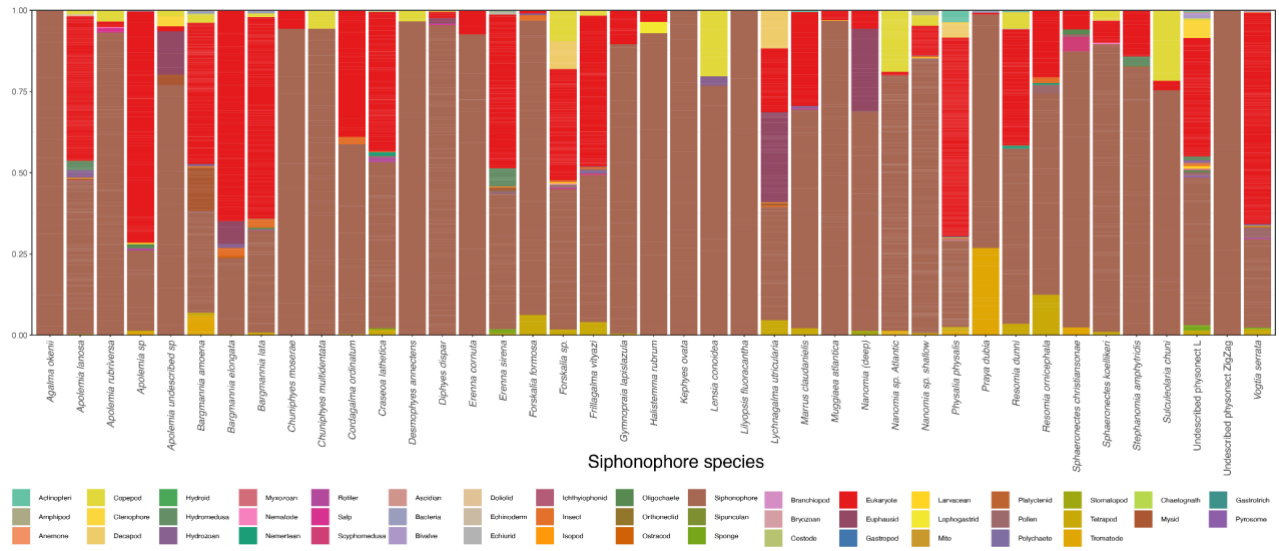

SM-Figure 6. Relative read log-abundance colored by OTU taxon for each species.

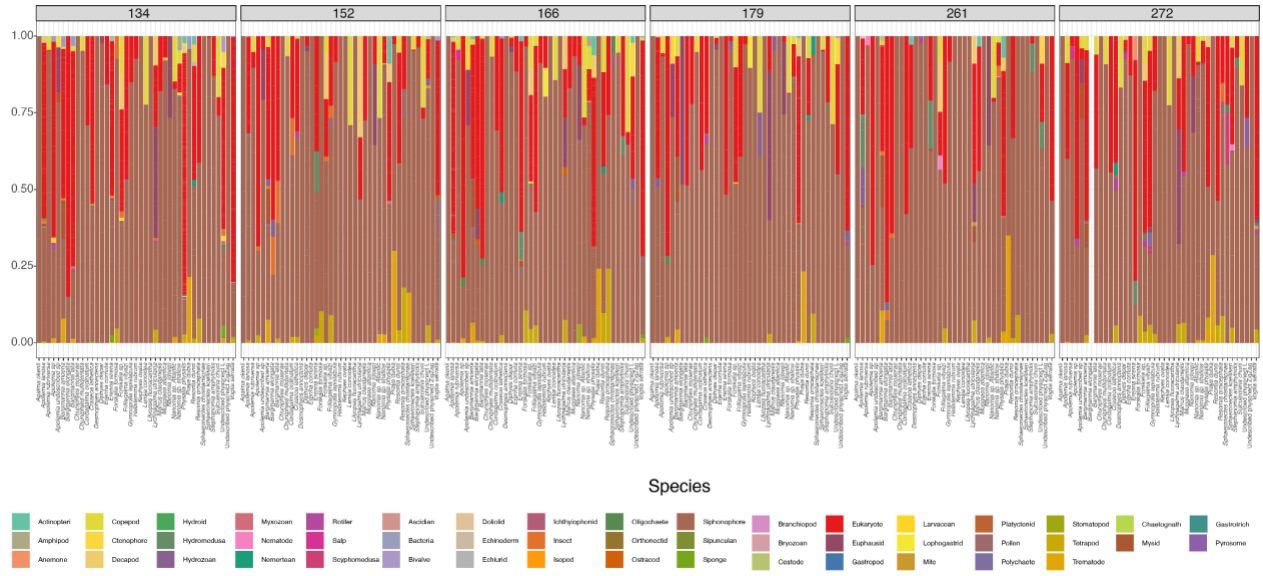

SM-Figure 7. Relative read log-abundance colored by OTU taxon for each species and barcode region.

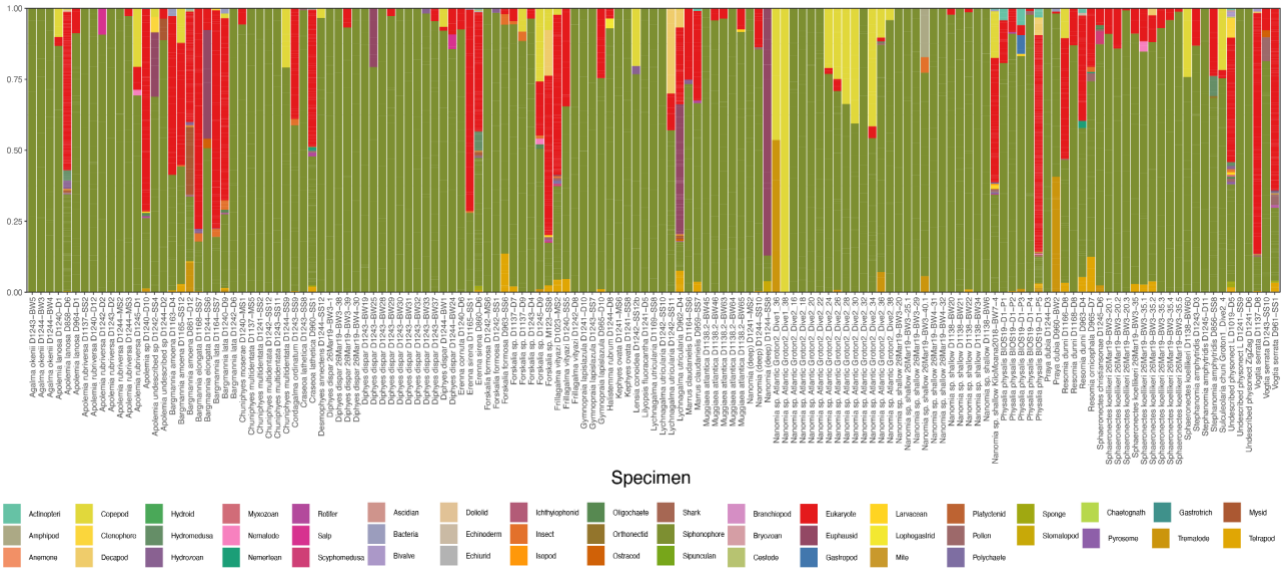

SM-Figure 8. Relative read log-abundance colored by OTU taxon for each specimen.

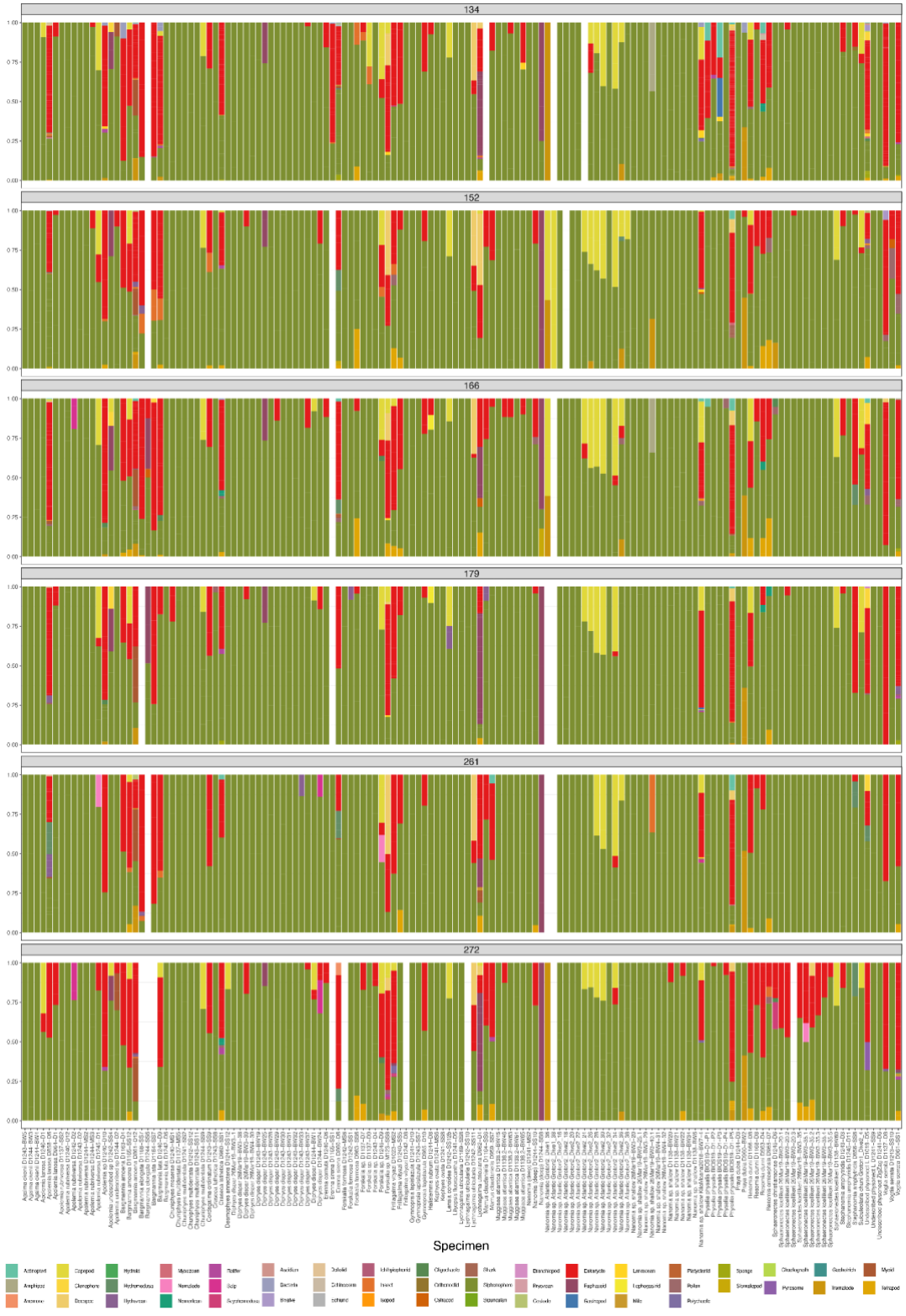

SM-Figure 9. Relative read log-abundance colored by OTU taxon for each specimen and barcode.

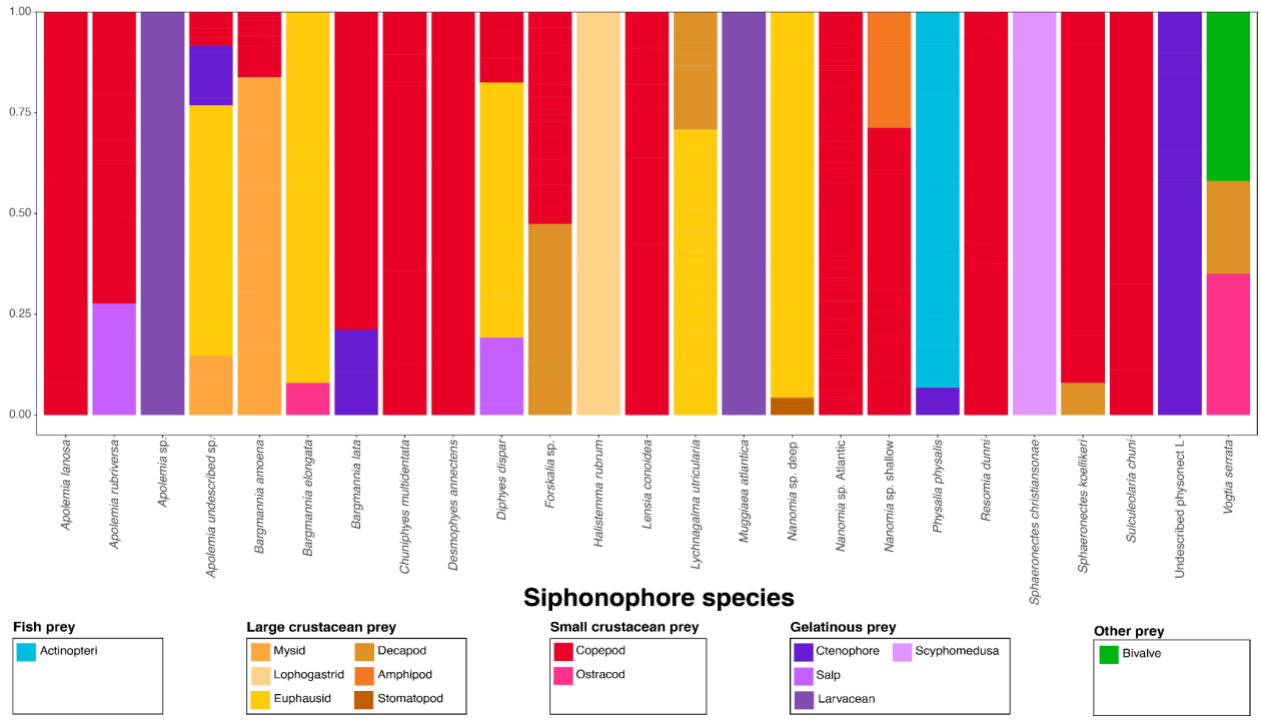

SM-Figure 10. Relative read log-abundance of prey colored by prey taxon for each siphonophore species.

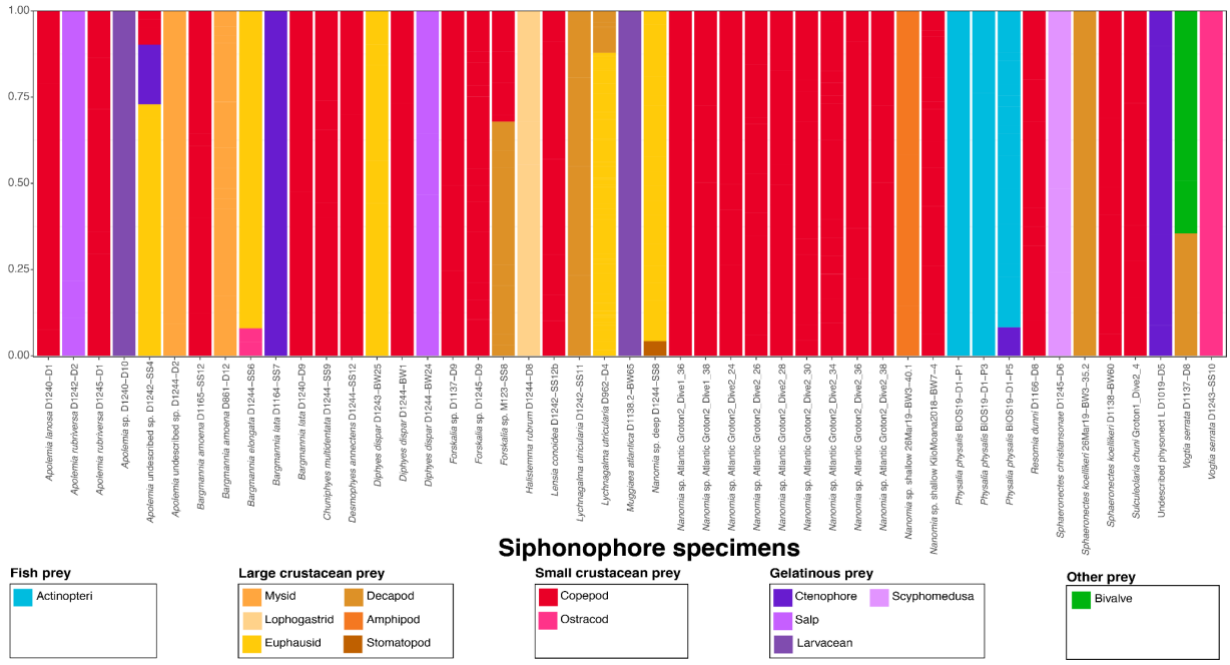

SM-Figure 11. Relative read log-abundance of prey colored by prey taxon for each siphonophore specimen.

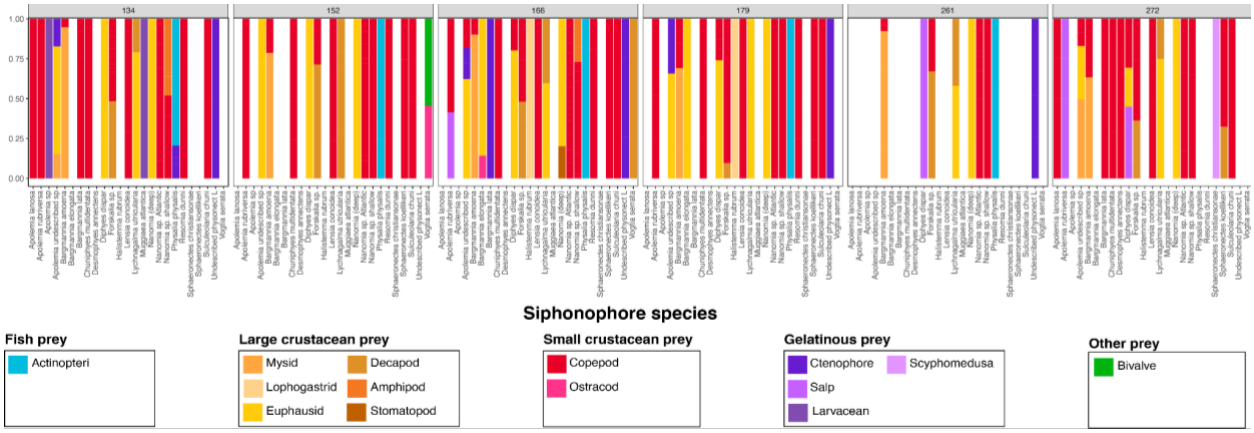

SM-Figure 12. Relative read log-abundance of prey colored by prey taxon for each siphonophore species and barcode.

SM-Table 1. Specimen collection metadata table specifying date, location, and depth where each animal was collected.

Specimen	Species	Collection date (Y-M-D)	Location	Coordinates	Depth (m)
BIOS19-D1-P1	*Physalia physalis*	2019-05-16	Atlantic Ocean, off Bermuda	32.33 N 64.65 W	0
BIOS19-D1-P2	*Physalia physalis*	2019-05-16	Atlantic Ocean, off Bermuda	32.35 N 64.62 W	0
BIOS19-D1-P3	*Physalia physalis*	2019-05-16	Atlantic Ocean, off Bermuda	32.35 N 64.62 W	0
BIOS19-D1-P4	*Physalia physalis*	2019-05-16	Atlantic Ocean, off Bermuda	32.36 N 64.58 W	0
BIOS19-D1-P5	*Physalia physalis*	2019-05-16	Atlantic Ocean, off Bermuda	32.38 N 64.59 W	0
D965-D7	*Resomia ornicephala*	2017-06-14	Pacific Ocean, off California	36.70 N 122.06 W	206
D1244-SS12	*Desmophyes annectens*	2020-02-01	Pacific Ocean, off California	33.25 N 118.31 W	212
D1241-MS2	*Nanomia sp.* deep	2020-01-29	Pacific Ocean, off California	35.21 N 121.33 W	238
D1244-D3	*Praya dubia*	2020-02-01	Pacific Ocean, off California	33.25 N 118.31 W	252
D1244-SS10	*Nanomia sp.* deep	2020-02-01	Pacific Ocean, off California	33.25 N 118.31 W	253
D1241-SS2	*Chuniphyes multidentata*	2020-01-29	Pacific Ocean, off California	35.21 N 121.33 W	267
D1242-MS6	*Forskalia formosa*	2020-01-30	Pacific Ocean, off California	33.85 N 119.65 W	290
D1243-SS11	*Chuniphyes multidentata*	2020-01-31	Pacific Ocean, off California	33.16 N 119.25 W	300
D1242-SS12	*Chuniphyes multidentata*	2020-01-30	Pacific Ocean, off California	33.85 N 119.65 W	302
D1242-SS12b	*Lensia conoidea*	2020-01-30	Pacific Ocean, off California	33.85 N 119.65 W	302
D1244-SS9	*Chuniphyes multidentata*	2020-02-01	Pacific Ocean, off California	33.25 N 118.31 W	310
D1241-D6	Physonectae sp. Z	2020-01-29	Pacific Ocean, off California	35.21 N 121.33 W	321
D1241-D5	*Lilyopsis fluoracantha*	2020-01-29	Pacific Ocean, off California	35.21 N 121.33 W	322
D1243-SS10	*Vogtia serrata*	2020-01-31	Pacific Ocean, off California	33.16 N 119.25 W	345
D1137-D9	*Forskalia sp.*	2019-03-22	Pacific Ocean, off California	36.70 N 122.06 W	347
D1137-D7	*Forskalia sp.*	2019-03-22	Pacific Ocean, off California	36.70 N 122.06 W	349
D1243-SS9	*Cordagalma ordinatum*	2020-01-31	Pacific Ocean, off California	33.16 N 119.25 W	364
D1023-MS2	*Frillagalma vityazi*	2018-05-05	Pacific Ocean, off California	35.93 N 124.00 W	379
D1243-D4	*Forskalia sp.*	2020-01-31	Pacific Ocean, off California	33.16 N 119.25 W	393
D1243-SS8	*Craseoa lathetica*	2020-01-31	Pacific Ocean, off California	33.16 N 119.25 W	399
D1243-SS7	*Gymnopraia lapislazula*	2020-01-31	Pacific Ocean, off California	33.16 N 119.25 W	400
D1244-D8	*Halistemma rubrum*	2020-02-01	Pacific Ocean, off California	33.25 N 118.31 W	402
D1244-SS8	*Nanomia sp.* deep	2020-02-01	Pacific Ocean, off California	33.25 N 118.31 W	402
D1245-D9	*Forskalia sp.*	2020-02-02	Pacific Ocean, off California	32.72 N 117.72 W	405
D963-SS6	*Forskalia formosa*	2017-06-12	Pacific Ocean, off California	36.60 N 122.15 W	411
D1241-D10	*Gymnopraia lapislazula*	2020-01-29	Pacific Ocean, off California	35.21 N 121.33 W	414
D1240-SS5	*Frillagalma vityazi*	2020-01-28	Pacific Ocean, off California	36.56 N 122.25 W	421
D964-D1	*Apolemia lanosa*	2017-06-13	Pacific Ocean, off California	36.80 N 122.00 W	430
D1168-SS7	*Bargmannia elongata*	2019-07-15	Pacific Ocean, off California	36.41 N 122.28 W	437
D1242-SS11	*Lychnagalma utricularia*	2020-01-30	Pacific Ocean, off California	33.85 N 119.65 W	448
D856-SS8	*Stephanomia amphytridis*	2016-06-11	Pacific Ocean, off California	36.50 N 122.30 W	450
D1169-SS8	*Lychnagalma utricularia*	2019-07-16	Pacific Ocean, off California	36.60 N 122.15 W	456
D1242-SS1	*Forskalia formosa*	2020-01-30	Pacific Ocean, off California	33.85 N 119.65 W	469
D962-D4	*Lychnagalma utricularia*	2017-06-11	Pacific Ocean, off California	36.44 N 122.28 W	484
D1242-D8	*Frillagalma vityazi*	2020-01-30	Pacific Ocean, off California	33.85 N 119.65 W	497
D1244-SS6	*Bargmannia elongata*	2020-02-01	Pacific Ocean, off California	33.25 N 118.31 W	500
D1242-SS10	*Lychnagalma utricularia*	2020-01-30	Pacific Ocean, off California	33.85 N 119.65 W	501
D1240-D12	*Apolemia rubriversa*	2020-01-28	Pacific Ocean, off California	36.56 N 122.25 W	521
D965-D10	*Gymnopraia lapislazula*	2017-06-14	Pacific Ocean, off California	36.70 N 122.06 W	523
D1241-SS9	Physonectae sp. L	2020-01-29	Pacific Ocean, off California	35.21 N 121.33 W	601
M123-SS8	*Forskalia sp.*	2018-11-10	Pacific Ocean, off Hawaii	24.48 N 160.37 W	615
D1241-MS6	*Kephyes ovata*	2020-01-29	Pacific Ocean, off California	35.21 N 121.33 W	650
D1241-SS8	*Kephyes ovata*	2020-01-29	Pacific Ocean, off California	35.21 N 121.33 W	650
D1240-D10	*Apolemia sp.*	2020-01-28	Pacific Ocean, off California	36.56 N 122.25 W	752
D1164-SS7	*Bargmannia lata*	2019-07-11	Pacific Ocean, off California	36.18 N 123.22 W	752
D1137-D8	*Vogtia serrata*	2019-03-22	Pacific Ocean, off California	36.70 N 122.06 W	766
D1137-MS5	*Chuniphyes multidentata*	2019-03-22	Pacific Ocean, off California	36.70 N 122.06 W	770
D1245-D11	*Stephanomia amphytridis*	2020-02-02	Pacific Ocean, off California	32.72 N 117.72 W	793
D1245-D1	*Apolemia rubriversa*	2020-02-02	Pacific Ocean, off California	32.72 N 117.72 W	797
D1244-MS3	*Apolemia rubriversa*	2020-02-01	Pacific Ocean, off California	33.25 N 118.31 W	816
D1244-MS2	*Apolemia rubriversa*	2020-02-01	Pacific Ocean, off California	33.25 N 118.31 W	834
D961-SS1	*Vogtia serrata*	2017-06-10	Pacific Ocean, off California	35.50 N 124.00 W	852
D1244-D2	*Apolemia sp.*	2020-02-01	Pacific Ocean, off California	33.25 N 118.31 W	862
D1240-D1	*Apolemia lanosa*	2020-01-28	Pacific Ocean, off California	36.56 N 122.25 W	884
D1245-D6	*Sphaeronectes christiansonae*	2020-02-02	Pacific Ocean, off California	32.72 N 117.72 W	891
D959-SS7	*Marrus claudanielis*	2017-06-08	Pacific Ocean, off California	35.93 N 122.93 W	1013
D963-D4	*Resomia dunni*	2017-06-12	Pacific Ocean, off California	36.60 N 122.15 W	1017
D1240-D9	*Bargmannia lata*	2020-01-28	Pacific Ocean, off California	36.56 N 122.25 W	1022
D858-D6	*Apolemia lanosa*	2016-06-13	Pacific Ocean, off California	36.33 N 122.90 W	1088
D1242-D6	*Bargmannia lata*	2020-01-30	Pacific Ocean, off California	33.85 N 119.65 W	1117
D1137-SS2	*Apolemia rubriversa*	2019-03-22	Pacific Ocean, off California	36.70 N 122.06 W	1129
D1243-D2	*Apolemia rubriversa*	2020-01-31	Pacific Ocean, off California	33.16 N 119.25 W	1201
D1019-D5	Physonectae sp. L	2018-05-02	Pacific Ocean, off California	36.59 N 122.53 W	1340

Specimen	Species	Collection date (Y-M-D)	Location	Coordinates	Depth (m)
D1240-D6	*Erenna cornuta*	2020-01-28	Pacific Ocean, off California	36.56 N 122.25 W	1352
D1240-MS1	*Chuniphyes moserae*	2020-01-28	Pacific Ocean, off California	36.56 N 122.25 W	1359
D1242-SS4	*Apolemia sp.*	2020-01-30	Pacific Ocean, off California	33.85 N 119.65 W	1388
D1164-SS6	*Marrus claudanielis*	2019-07-11	Pacific Ocean, off California	36.18 N 123.22 W	1393
D1243-D3	*Stephanomia amphytridis*	2020-01-31	Pacific Ocean, off California	33.16 N 119.25 W	1460
D960-SS1	*Craseoa lathetica*	2017-06-09	Pacific Ocean, off California	35.49 N 123.99 W	1708
D860-D6	*Erenna sirena*	2016-06-15	Pacific Ocean, off California	36.33 N 122.90 W	2145
D1165-SS1	*Erenna sirena*	2019-07-12	Pacific Ocean, off California	36.18 N 123.22 W	2243
D1166-D8	*Resomia dunni*	2019-07-13	Pacific Ocean, off California	35.26 N 125.02 W	2953
D1165-SS12	*Bargmannia amoena*	2019-07-12	Pacific Ocean, off California	36.18 N 123.22 W	3647
D1243-BW5	*Agalma okenii*	2020-01-31	Pacific Ocean, off California	33.16 N 119.25 W	0-20
D1244-BW3	*Agalma okenii*	2020-02-01	Pacific Ocean, off California	33.25 N 118.31 W	0-20
D1244-BW4	*Agalma okenii*	2020-02-01	Pacific Ocean, off California	33.25 N 118.31 W	0-20
26Mar19-BW3-1	*Diphyes dispar*	2019-03-26	Pacific Ocean, off California	36.80 N 122.41 W	0-20
26Mar19-BW3-38	*Diphyes dispar*	2019-03-26	Pacific Ocean, off California	36.80 N 122.41 W	0-20
26Mar19-BW3-39	*Diphyes dispar*	2019-03-26	Pacific Ocean, off California	36.80 N 122.41 W	0-20
26Mar19-BW4-30	*Diphyes dispar*	2019-03-26	Pacific Ocean, off California	36.80 N 122.41 W	0-20
D1243-BW19	*Diphyes dispar*	2020-01-31	Pacific Ocean, off California	33.16 N 119.25 W	0-20
D1243-BW25	*Diphyes dispar*	2020-01-31	Pacific Ocean, off California	33.16 N 119.25 W	0-20
D1243-BW28	*Diphyes dispar*	2020-01-31	Pacific Ocean, off California	33.16 N 119.25 W	0-20
D1243-BW29	*Diphyes dispar*	2020-01-31	Pacific Ocean, off California	33.16 N 119.25 W	0-20
D1243-BW30	*Diphyes dispar*	2020-01-31	Pacific Ocean, off California	33.16 N 119.25 W	0-20
D1243-BW31	*Diphyes dispar*	2020-01-31	Pacific Ocean, off California	33.16 N 119.25 W	0-20
D1243-BW32	*Diphyes dispar*	2020-01-31	Pacific Ocean, off California	33.16 N 119.25 W	0-20
D1243-BW33	*Diphyes dispar*	2020-01-31	Pacific Ocean, off California	33.16 N 119.25 W	0-20
D1243-BW37	*Diphyes dispar*	2020-01-31	Pacific Ocean, off California	33.16 N 119.25 W	0-20
D1244-BW1	*Diphyes dispar*	2020-02-01	Pacific Ocean, off California	33.25 N 118.31 W	0-20
D1244-BW24	*Diphyes dispar*	2020-02-01	Pacific Ocean, off California	33.25 N 118.31 W	0-20
D1138.2-BW45	*Muggiaea atlantica*	2019-03-24	Pacific Ocean, off California	36.46 N 122.53 W	0-20
D1138.2-BW46	*Muggiaea atlantica*	2019-03-24	Pacific Ocean, off California	36.46 N 122.53 W	0-20
D1138.2-BW63	*Muggiaea atlantica*	2019-03-24	Pacific Ocean, off California	36.46 N 122.53 W	0-20
D1138.2-BW64	*Muggiaea atlantica*	2019-03-24	Pacific Ocean, off California	36.46 N 122.53 W	0-20
D1138.2-BW65	*Muggiaea atlantica*	2019-03-24	Pacific Ocean, off California	36.46 N 122.53 W	0-20
Groton2_Dive1_36	*Nanomia sp.* Atlantic	2020-10-04	Atlantic Ocean, off Block Island	40.97 N 71.66 W	0-20
Groton2_Dive1_38	*Nanomia sp.* Atlantic	2020-10-04	Atlantic Ocean, off Block Island	40.97 N 71.66 W	0-20
Groton2_Dive2_16	*Nanomia sp.* Atlantic	2020-10-04	Atlantic Ocean, off Block Island	40.97 N 71.66 W	0-20
Groton2_Dive2_18	*Nanomia sp.* Atlantic	2020-10-04	Atlantic Ocean, off Block Island	40.97 N 71.66 W	0-20
Groton2_Dive2_20	*Nanomia sp.* Atlantic	2020-10-04	Atlantic Ocean, off Block Island	40.97 N 71.66 W	0-20
Groton2_Dive2_22	*Nanomia sp.* Atlantic	2020-10-04	Atlantic Ocean, off Block Island	40.97 N 71.66 W	0-20
Groton2_Dive2_24	*Nanomia sp.* Atlantic	2020-10-04	Atlantic Ocean, off Block Island	40.97 N 71.66 W	0-20
Groton2_Dive2_26	*Nanomia sp.* Atlantic	2020-10-04	Atlantic Ocean, off Block Island	40.97 N 71.66 W	0-20
Groton2_Dive2_28	*Nanomia sp.* Atlantic	2020-10-04	Atlantic Ocean, off Block Island	40.97 N 71.66 W	0-20
Groton2_Dive2_30	*Nanomia sp.* Atlantic	2020-10-04	Atlantic Ocean, off Block Island	40.97 N 71.66 W	0-20
Groton2_Dive2_32	*Nanomia sp.* Atlantic	2020-10-04	Atlantic Ocean, off Block Island	40.97 N 71.66 W	0-20
Groton2_Dive2_34	*Nanomia sp.* Atlantic	2020-10-04	Atlantic Ocean, off Block Island	40.97 N 71.66 W	0-20
26Mar19-BW3-20	*Nanomia sp.* shallow	2019-03-26	Pacific Ocean, off California	36.80 N 122.41 W	0-20
26Mar19-BW3-25.1	*Nanomia sp.* shallow	2019-03-26	Pacific Ocean, off California	36.80 N 122.41 W	0-20
26Mar19-BW3-29	*Nanomia sp.* shallow	2019-03-26	Pacific Ocean, off California	36.80 N 122.41 W	0-20
26Mar19-BW3-40.1	*Nanomia sp.* shallow	2019-03-26	Pacific Ocean, off California	36.80 N 122.41 W	0-20
26Mar19-BW4-31	*Nanomia sp.* shallow	2019-03-26	Pacific Ocean, off California	36.80 N 122.41 W	0-20
26Mar19-BW4-32	*Nanomia sp.* shallow	2019-03-26	Pacific Ocean, off California	36.80 N 122.41 W	0-20
D1138-BW20	*Nanomia sp.* shallow	2019-03-24	Pacific Ocean, off California	36.38 N 122.67 W	0-20
D1138-BW21	*Nanomia sp.* shallow	2019-03-24	Pacific Ocean, off California	36.38 N 122.67 W	0-20
D1138-BW22	*Nanomia sp.* shallow	2019-03-24	Pacific Ocean, off California	36.38 N 122.67 W	0-20
D1138-BW34	*Nanomia sp.* shallow	2019-03-24	Pacific Ocean, off California	36.38 N 122.67 W	0-20
D1138-BW6	*Nanomia sp.* shallow	2019-03-24	Pacific Ocean, off California	36.38 N 122.67 W	0-20
KiloMoana2018-	*Nanomia sp.* shallow	2018-11-09	Pacific Ocean, off Hawaii	19.58 N 156.31 W	0-20
D960-BW2	*Praya dubia*	2017-06-09	Pacific Ocean, off California	35.49 N 123.99 W	0-20
26Mar19-BW3-20.1	*Sphaeronectes koellikeri*	2019-03-26	Pacific Ocean, off California	36.80 N 122.41 W	0-20
26Mar19-BW3-20.2	*Sphaeronectes koellikeri*	2019-03-26	Pacific Ocean, off California	36.80 N 122.41 W	0-20
26Mar19-BW3-20.3	*Sphaeronectes koellikeri*	2019-03-26	Pacific Ocean, off California	36.80 N 122.41 W	0-20
26Mar19-BW3-35	*Sphaeronectes koellikeri*	2019-03-26	Pacific Ocean, off California	36.80 N 122.41 W	0-20
26Mar19-BW3-35.1	*Sphaeronectes koellikeri*	2019-03-26	Pacific Ocean, off California	36.80 N 122.41 W	0-20
26Mar19-BW3-35.2	*Sphaeronectes koellikeri*	2019-03-26	Pacific Ocean, off California	36.80 N 122.41 W	0-20
26Mar19-BW3-35.3	*Sphaeronectes koellikeri*	2019-03-26	Pacific Ocean, off California	36.80 N 122.41 W	0-20
26Mar19-BW3-35.4	*Sphaeronectes koellikeri*	2019-03-26	Pacific Ocean, off California	36.80 N 122.41 W	0-20
26Mar19-BW3-35.5	*Sphaeronectes koellikeri*	2019-03-26	Pacific Ocean, off California	36.80 N 122.41 W	0-20
D1138-BW60	*Sphaeronectes koellikeri*	2019-03-24	Pacific Ocean, off California	36.38 N 122.67 W	0-20
Groton1_Dive2_4	*Sulculeolaria sp.*	2020-08-20	Pacific Ocean, off California	41.06 N 71.70 W	0-20
D1168-D4	Physonect (lost record)	2019-07-10	Pacific Ocean, off California	36.41 N 122.30 W	935

Specimen	Species	Collection date (Y-M-D)	Location	Coordinates	Depth (m)
D861-D12	*Bargmannia amoena*	2016-06-16	Pacific Ocean, off California	36.65 N 122.06 W	1323

SM-Table 2. Plankton net trawl collection metadata table specifying date, location, and depth where each prey field sample was collected.

Expedition	Date	Dive #	Trawl #	Type of net	Mesh size (µm)	Net frame area (m2)	Distance (m)	Volume (m3)	Start time	End time	Depth range (m)	Latitude (N)	Longitude (W)
WF_March2019	**03/22/19**	D1137	T1	Minitucker	1000	4	NA	NA	19:39	20:15	0-340	36.70	122.06
WF_March2019	**03/24/19**	D1138	BWT1	Hand net	200	0.19634	NA	NA	NA	NA	0-5	36.38	122.67
WF_March2019	**03/26/19**	26Mar19-BW3	BWT3	Hand net	200	0.19634	NA	NA	NA	NA	0-20	36.80	122.41
WF_March2019	**03/26/19**	26Mar19-BW4	BWT4	Hand net	200	0.19634	NA	NA	NA	NA	0-20	36.80	122.41
BIOS19	**05/16/19**	D1	Trawl1	Hand net	200	0.7854	3310.16	2600	14:00	14:10	0-3	32.33	64.65
WF_Jan2020	**02/01/2020**	D1244	MT1	Hand net	200	0.19634	20	4	10:00	10:05	0-20	33.25	118.31
Groton_1	**08/20/2020**	BW2	Trawl2	Hand net	500	0.7854	49.112	39	11:36	NA	0-20	41.06	71.69
Groton_2	**10/04/2020**	Dive_1	Trawl1	Hand net	500	0.7854	52.136	41	11:45	NA	0-20	40.97	-71.68